Inorganic Chemistry

Article

pubs.acs.org/IC

Synthesis, Spectral, and Electrochemical Studies of Electronically Tunable β-Substituted Porphyrins with Mixed Substituent Pattern

Ravi Kumar and Muniappan Sankar*

Department of Chemistry, Indian Institute of Technology Roorkee, Roorkee - 247667, India

Supporting Information

ABSTRACT: Two new families of porphyrins with mixed substituent pattern, viz. 2-nitro-12,13-disubstituted-*meso*-tetraphenylporphyrins ($H_2TPP(NO_2)X_2$, X = Ph, phenylethynyl (PE), 2-thienyl (Th), Br, and CN) and 2-nitro-7,8,12,13,17,18-hexasubstituted-*meso*-tetraphenylporphyrins ($H_2TPP(NO_2)X_6$, X = Br, Ph, PE, and Th), and their metal (Co(II), Ni(II), Cu(II), and Zn(II)) complexes have been synthesized and characterized. $H_2TPP(NO_2)X_6$ exhibited remarkable red shift in the Soret band (45−70 nm) and longest wavelength band, $Q_x(0,0)$ (65−90 nm), as compared to $H_2TPP(NO_2)$. Single-crystal structures of $MTPP(NO_2)X_2$ (M = Zn(II) and Ni(II); X = Br, Ph, and PE) showed quasi-planar conformation, whereas $H_2TPP(NO_2)Th_2$ and $NiTPP(NO_2)Br_6$ exhibited moderate and highly nonplanar saddle-shape conformations, respectively. Further, DFT fully optimized geometries of $H_2TPP(NO_2)X_2$ and $H_2TPP(NO_2)X_6$ revealed moderate and severe saddle-shape nonplanar conformations, respectively. The imino proton resonances of $H_2TPP(NO_2)X_6$ are significantly downfield shifted ($\Delta\delta$ = 1.10−1.80 ppm) relative to $H_2TPP(NO_2)$. Mixed substituted highly nonplanar porphyrins exhibited higher protonation and deprotonation constants relative to H_2TPPX_8 (X = Cl and Br). The redox tunability was achieved by introducing electron donor (Ph and Th) and acceptor (PE, Br, and CN) groups on the $MTPP(NO_2)$ backbone. The unusual variation in the spectral and electrochemical redox properties of mixed substituted porphyrins are interpreted in terms of both an inductive and a resonance interaction of substituents on the porphyrin π-system as well as nonplanarity of the macrocycle.

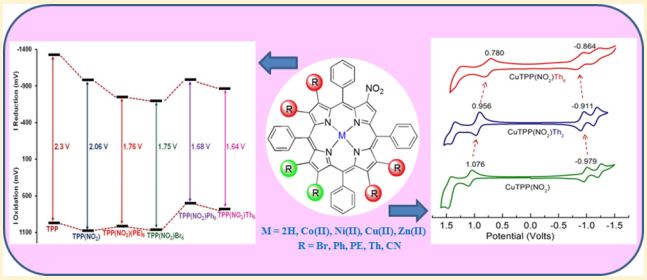

INTRODUCTION

Porphyrinoids play a vital role in biological systems, and their synthesis arouses continuing interest in biological, material, and inorganic chemistry.[1] The advantage of using porphyrin ligands is that they are conformationally flexible and can adopt a range of nonplanar conformations needed for a variety of biological functions.[1,2] Porphyrins and their metal complexes were used in catalysis,[3] dye-sensitized solar cells (DSSC),[4] photodynamic therapy (PDT),[5] molecular sensors,[6] nonlinear optical (NLO) materials,[7] and sorbents[8] due to their outstanding properties, such as high chemical and thermal stability, strong absorption in the visible region, and flexible architectural modification to tailor physicochemical and optoelectronic parameters. The β-functionalization of *meso*-tetraphenylporphyrins is of great interest since the electronic properties of the porphyrin macrocycle can be altered by small changes in the substituents.[9] Moreover, the substituents at the β positions of the porphyrins exert much larger steric and electronic effects on the porphyrin π-system[1e,f,10] than substituents at the *meso*-aryl positions. The redox properties of the natural and synthetic porphyrins depend upon various factors such as core structure, the type and location of electron-donating or -withdrawing substituents, the electronic nature and oxidation state of the central metal ion, and the type and number of bound axial ligands.[10] The β-nitration of the porphyrin ring is of special interest since the nitro groups are versatile and can be converted into several other functional groups.[11] β-Nitroporphyrins exhibited interesting catalytic,[12a] photophysical,[12b] and nonlinear optical properties.[12c] Further, β-bromosubstituted tetraarylporphyrins are useful substrates for nucleophilic aromatic substitutions with cyanides,[13a] thiolates,[13b] and benzaldoximate[13c] or in palladium(0)-mediated cross-coupling reactions with arylboronic acids,[13d−f] alkynes,[13g] alkenes,[13h] and organozinc[13i] or organotributyltin reagents.[13j−n] Modification utilizing Pd-catalyzed reactions of carbon−carbon bond formation is widely used for synthesis of new porphyrin systems of various architectures.[13,14] The *meso*-substituted push−pull porphyrins have been widely explored due to their relative ease of synthesis, whereas studies on β-pyrrole mixed substituted or push−pull porphyrins are very much limited due to lack of synthetic methodologies.[15] Introduction of sterically demanding substituents at the periphery leads to a significantly nonplanar macrocycle conformation.[16] Perhalo substitution also affects the photophysical and electrochemical properties of the porphyrin π-system extensively.[17] An increase in the number of substituents enhances the steric crowding and thus induces enhanced steric repulsive interaction among the peripheral substituents leading

Received: June 2, 2014
Published: November 20, 2014

to the nonplanarity of the macrocycle.[18] On the other hand, the two-photon absorption (TPA) cross section of push−pull Zn(II) porphyrin with donor and acceptor groups at the β or *meso* position of the porphyrin ring exhibited a much larger σ_{TPA} value than that of homo-substituted porphyrins.[19] Development of new materials with enhanced NLO responses is of great scientific interest due to their potential applications in optical limiting devices, optical communications, and optical data processing. Asymmetrically substituted porphyrins constitute a promising group of NLO compounds due to high nonlinearities upon irradiation with high-intensity laser light.[7] The main advantage of porphyrins is their chemical versatility, which provides a tool for tailoring the linear and NLO properties for specific applications.[7,20] One field of potential use of NLO active porphyrinic dyes is broad-band optical limiting (OL),[7e,20] which aims for protection of human eyes and sensitive optical elements against accidental exposure to high-energy laser beams. Herein, we focused on synthesizing the mixed substituted porphyrins in order to tune the electronic spectral and electrochemical redox properties of the porphyrin π-system. In general, the syntheses and properties of porphyrins with mixed antipodal β-substituents are largely unexamined.[21] With these objectives, we report the synthesis, structural, physicochemical, and electrochemical redox properties of two new families of porphyrins with mixed substituent pattern, viz. 2-nitro-12,13-disubstituted-5,10,15,20-tetraphenylporphyrins ($H_2TPP(NO_2)X_2$, X = Ph, phenylethynyl (PE), 2-thienyl (Th), Br, and CN) and 2-nitro-7,8,12,13,17,18-hexasubstituted-5,10,15,20-tetraphenylporphyrins ($H_2TPP(NO_2)X_6$, X = Br, Ph, PE, and Th), and their metal (Co(II), Ni(II), Cu(II) and Zn(II)) complexes (Chart 1). To the best of our knowledge,

Chart 1. Molecular Structures of Porphyrins with Mixed Substituent Pattern

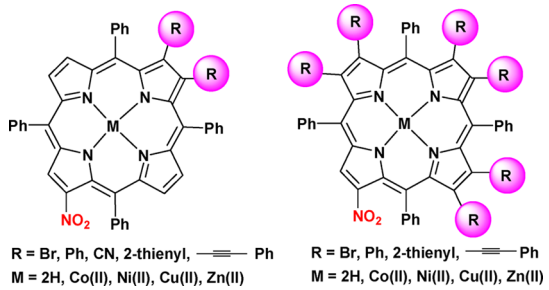

the protonation and deprotonation studies, ^{1}H NMR spectral features, and electrochemical redox properties of β-pyrrole tri- and heptasubstituted *meso*-TPPs with mixed substituent pattern and their metal complexes have not been studied so far.

RESULTS AND DISCUSSION

Synthesis and Characterization. Two new families of β-pyrrole mixed substituted porphyrins, viz. β-tri- and heptasubstituted *meso*-tetraphenylporphyrins ($MTPP(NO_2)X_n$, n = 2, 6), were synthesized and characterized, Scheme 1. 2-Nitro-*meso*-TPPs are versatile precursors in porphyrin chemistry due to their excellent stability toward demetalation/metalation sequences[21c] and can be prepared in high yields (70−80%). The regioselective bromination of 2-nitro-*meso*-TPP afforded 2-nitro-12,13-dibromo-*meso*-TPP ($H_2TPP(NO_2)Br_2$), which was further utilized for Pd-catalyzed coupling reactions. $H_2TPP(NO_2)Br_2$ was subjected to Suzuki coupling using phenylboronic acid, affording $H_2TPP(NO_2)Ph_2$ with 71% yield. In general, β-substituted 2-thienyl porphyrins were prepared using Stille coupling reactions[13j−n] by reacting bromoporphyrins with expensive tributylthienylstannane. We synthesized the same porphyrins via Suzuki coupling reaction using inexpensive 2-thienylboronic acid with yields of 50−60%. $H_2TPP(NO_2)Br_2$ was subjected to Stille coupling reaction using tributylphenylethynylstannane in order to get $H_2TPP(NO_2)(PE)_2$. $NiTPP(NO_2)Br_2$ was also reacted with CuCN in quinoline to afford $NiTPP(NO_2)(CN)_2$ with 61% yield, which was further demetalated using H_2SO_4 to get $H_2TPP(NO_2)(CN)_2$.

The $CuTPP(NO_2)$ was hexabrominated using 10 equiv of freshly recrystallized NBS by refluxing in 1,2-dichloroethane at 80 °C for 16 h with 80% yield.[21c] Then $H_2TPP(NO_2)Br_6$ was obtained by acid demetalation of $CuTPP(NO_2)Br_6$ under mild conditions, which was subjected to Suzuki cross-coupling reactions to afford $H_2TPP(NO_2)Ph_6$ and $H_2TPP(NO_2)Th_6$ with good yields (60−70%). $H_2TPP(NO_2)(PE)_6$ was obtained via Stille coupling in 55% yield using a similar procedure to that of $H_2TPP(NO_2)(PE)_2$. Attempts to prepare $MTPP(NO_2)(CN)_6$ failed by reacting $NiTPP(NO_2)Br_6$ with CuCN and end up with degraded products. Metal complexes (Co(II), Cu(II), and Zn(II)) were prepared by reacting free base porphyrins with corresponding metal acetate hydrates (10 equiv) in refluxing $CHCl_3/CH_3OH$ mixture for 30 min, whereas Ni(II) complexes were synthesized using nickel acetate in refluxing DMF.[22a] Synthesized porphyrins were characterized by UV−vis, fluorescence, ^{1}H NMR, and mass spectroscopic techniques, elemental analysis, and single-crystal X-ray studies. Detailed synthetic procedures are described in the Supporting Information.

Crystal Structure Discussion. Crystallographic data of $NiTPP(NO_2)Ph_2(Py)$, $ZnTPP(NO_2)(PE)_2(CH_3OH)$, $ZnTPP(NO_2)Br_2(CH_3OH)$, $NiTPP(NO_2)Br_6$, and $H_2TPP(NO_2)(Th)_2\cdot CH_3OH\cdot H_2O$ are listed in Table S1, Supporting Information. ORTEP views (top and side) of $H_2TPP(NO_2)(Th)_2$ and $NiTPP(NO_2)Br_6$ are shown in Figure 1. The top and side ORTEP views for $MTPP(NO_2)X_2$ (M = Ni(II) and Zn(II); X = Ph, PE, and Br) are shown in Figure S1, Supporting Information. Selected average bond lengths and bond angles of these five porphyrins are listed in Table S2, Supporting Information. The observed bond distances and bond angles in these porphyrins are similar to those reported in the literature.[2d,e,22b,c] The nonplanarity of the porphyrin core is induced by the steric repulsion among the peripheral substituents, which enforces the relief of the strain through bond lengths and angles. The C−C bond distances of the β-pyrrole carbons (C_β−C_β bond lengths) bearing three β-substituents in these porphyrins are longer than that of $C_{\beta'}$−$C_{\beta'}$ distances where antipodal pyrroles bear no substitution (Table S2, Supporting Information). One would anticipate varying degrees of nonplanar conformations for mixed substituted porphyrins, since they bear substituents of different sizes which results in an increase in C_β−C_α−C_m angles with concomitant decrease in the N−C_α−C_m and M−N−C_α angles (Table S2, Supporting Information). The pyrrole groups of $H_2TPP(NO_2)(Th)_2$ are tilted alternatively up and down from the mean plane formed by the porphyrin macrocycle, and the β-substituents (nitro and 2-thienyl groups) on the opposite pyrrole units are tilted toward one face of the porphyrin. The 2-thienyl groups are oriented trans to each other in order to minimize the repulsions between the lone pairs. The displacement of atoms from the mean plane (Δ24) clearly shows the

dx.doi.org/10.1021/ic501259g | Inorg. Chem. 2014, 53, 12706−12719

Scheme 1. Synthetic Routes for Various Mixed Substituted Porphyrins

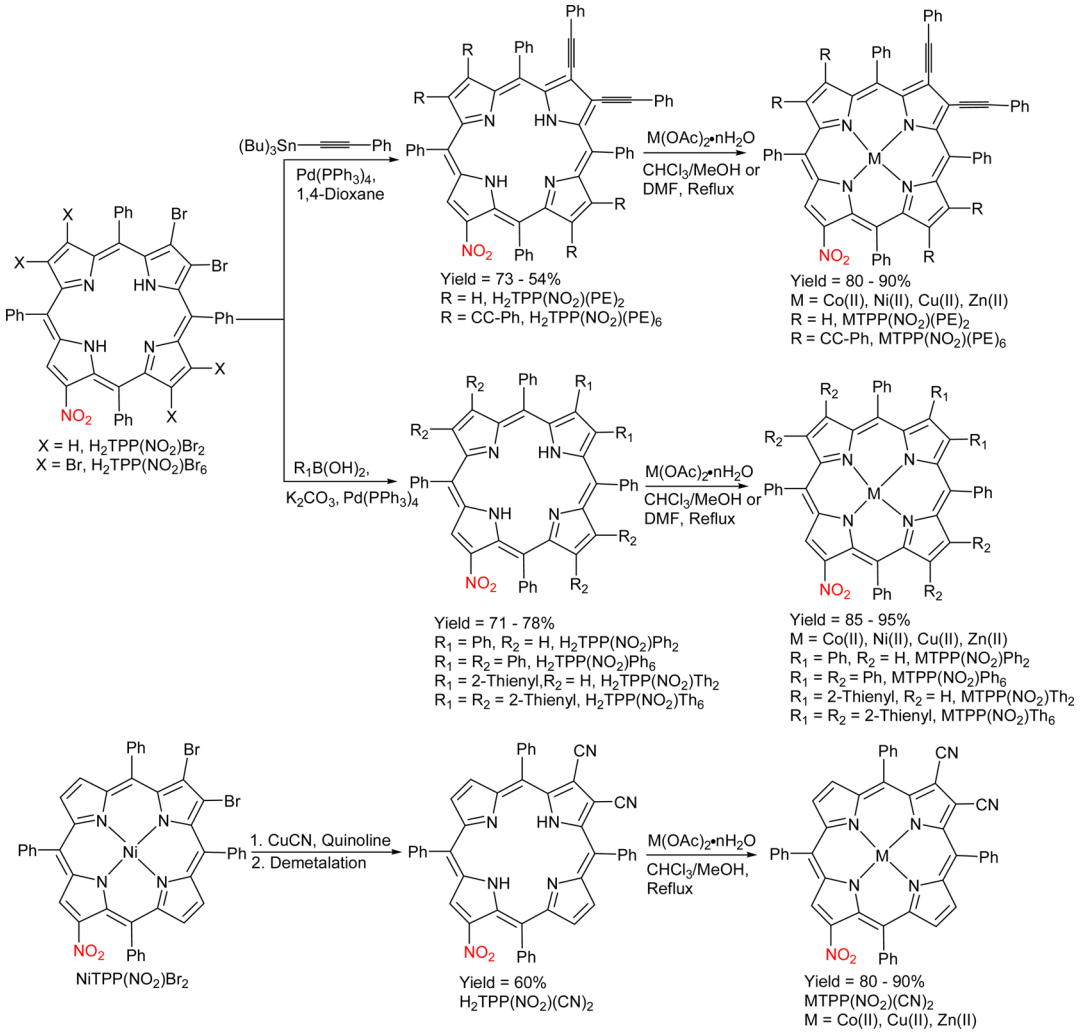

saddle conformation of the core (Figure 1). This is evident from the mean plane displacement of the β-pyrrole carbons (ΔC_β) and the *meso*-carbons from the mean plane (Figure 1c). The magnitude of the displacement of the β-pyrrole carbons (ΔC_β) of $H_2TPP(NO_2)(Th)_2$ was found to be $\pm$0.75 Å, which is significantly higher than that reported for H_2TPPBr_2 (ΔC_β = $\pm$ 0.209 Å) but lower than that of H_2TPPBr_6 (ΔC_β = $\pm$ 0.903 Å).[21c] Notably, the inner core imino protons (NH) are hydrogen bonded with pyrrole nitrogens, which are evidenced from the distance between the shortest N···N of 2.908 Å. The nitro group of $H_2TPP(NO_2)(Th)_2$ is interacting with the pyrrole moiety of another porphyrin unit with a distance of 3.217 Å exhibiting donor–acceptor interactions. Further, the oxygen of the NO_2 group has van der Waals interactions with the aromatic CH of thienyl and phenyl groups (O···C distances of 3.3–3.6 Å). The steric crowding between the β-substituents and the *meso*-phenyl rings as well as the supramolecular interactions are responsible for the nonplanar conformation of the porphyrin macrocycle in $H_2TPP(NO_2)(Th)_2$. Notably, $NiTPP(NO_2)Br_6$ has a severe saddle-shape conformation (Figure 1d and 1e) with displacement of the β-pyrrole carbons (ΔC_β = $\pm$ 1.10 Å). This is further supported by the increment in C_β–C_α–C_m angles (~127°) with concomitant decrement in the N–C_α–C_m (~123°) and M–N–C_α (~125°) angles along with larger C_β–C_β and $C_{\beta'}$–$C_{\beta'}$ bond lengths (1.34–1.35 Å). Ni(II) ion is in square planar geometry and about 0.035 Å above the mean plane. The longer M–N bond length as compared to M–N′ in $MTPP(NO_2)X_n$ (Table S2, Supporting Information) is possibly due to the electron-withdrawing effect of peripheral β-substitutents. It is known from the literature that $ZnTPPBr_4$, $ZnTPP(Ph)_4Br_4$, $NiTPPBr_4(CN)_4$, and $NiTPP(Ph)_4(CN)_4$ structures exhibited longer M–N distances due to the presence of the electron-withdrawing groups, which reduce the electron density on imino nitrogens.[21b,e] The methyl group of the axially coordinated CH_3OH in $ZnTPP(NO_2)(PE)_2$ shows some positional disorder. It is noteworthy that the Zn(II) ion is about 0.295 Å above the mean plane, which is higher than that of $ZnTPP(NO_2)Br_2(CH_3OH)$ complex (0.237 Å). Notably, five-coordinated Ni(II) ion in $NiTPP(NO_2)Ph_2(Py)$ is 0.397 Å above the mean plane of the porphyrin core. Moreover, the N–M–N and N′–M–N′ angles (161–170°) are deviated from 180°, indicating the nonplanar conformation of the M–$(N)_4$ core. The magnitude of the displacement of the β-pyrrole carbons (ΔC_β = $\pm$ 0.16 Å) in $NiTPP(NO_2)Ph_2(Py)$ and $ZnTPP(NO_2)Br_2(CH_3OH)$ is slightly higher than that of $ZnTPP(NO_2)(PE)_2(CH_3OH)$ (ΔC_β = $\pm$ 0.072 Å). Hence, the above-mentioned metalloporphyrins ($MTPP(NO_2)X_2$) show quasi-planar conformations. Moreover, $ZnTPP(NO_2)X_2(CH_3OH)$ (X = Br, PE) has dimeric structure through the hydrogen bonding interactions between the coordinated

dx.doi.org/10.1021/ic501259g | *Inorg. Chem.* 2014, 53, 12706–12719

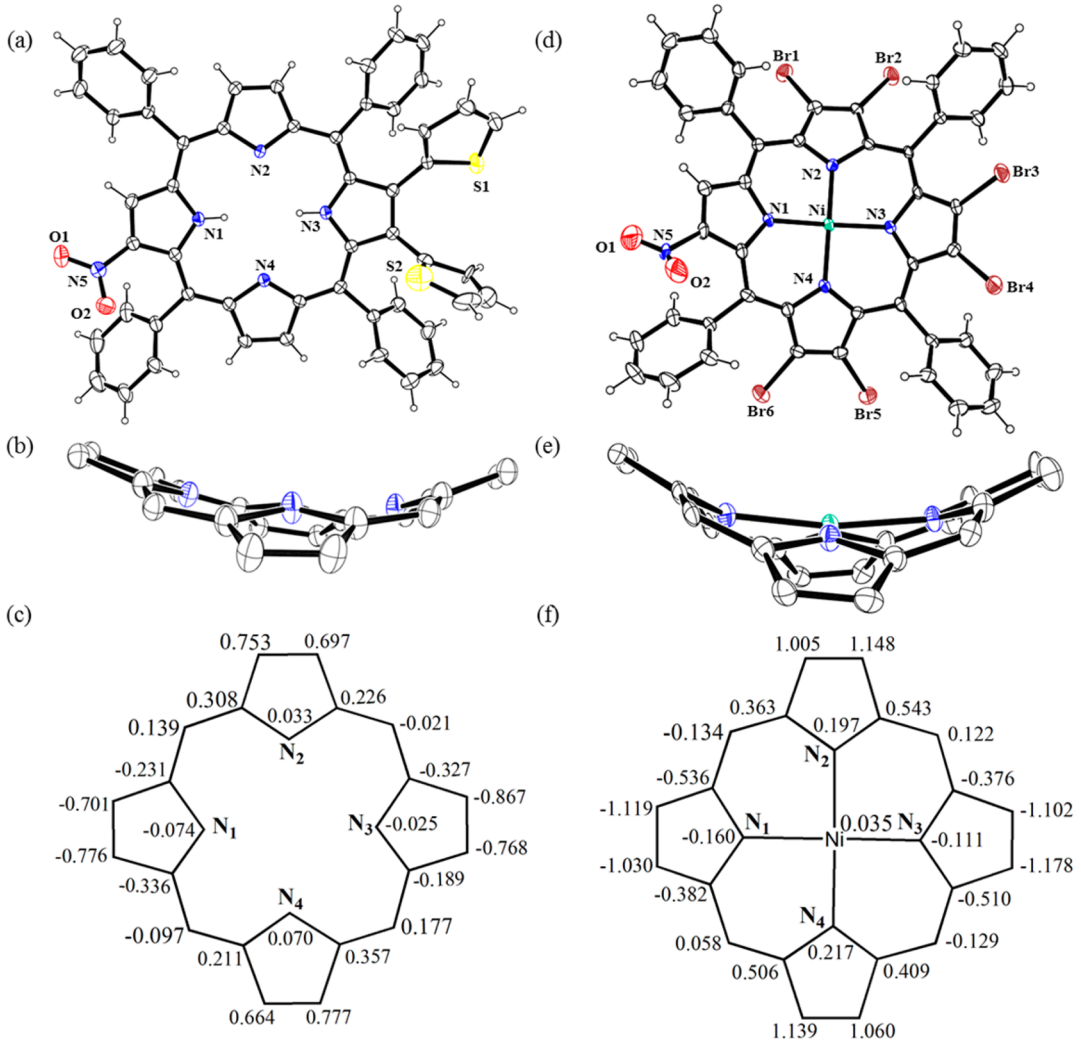

Figure 1. ORTEP diagrams showing top and side views of $H_2TPP(NO_2)(Th)_2$ (a and b) and $NiTPP(NO_2)Br_6$ (d and e), respectively. Solvates are not shown for clarity, and in side view, the β-substituents and *meso*-phenyl groups are not shown for clarity. (c and f) Displacement of porphyrin-core atoms (in Angstroms) from the mean plane for $H_2TPP(NO_2)(Th)_2$ and $NiTPP(NO_2)Br_6$, respectively.

methanol with the nitro group of the another porphyrin units with the shortest O···O distance of 2.874 (5) Å. The closest distance between the metalloporphyrin units is more than 3.40 Å, indicating that the steric crowding between the β-substituents and the *meso*-phenyl groups is responsible for the nonplanar conformation rather than the $\pi-\pi$ interactions between the macrocyclic π-systems. From single-crystal structure analysis, it is observed that $H_2TPP(NO_2)Th_2$ and $ZnTPP(NO_2)Br_6$ exhibit moderate and severe nonplanar saddle-shape conformations, respectively. Unfortunately, we were unable to crystallize other free bases and metal complexes of mixed substituted porphyrins, and hence, we carried out full geometry optimization using DFT studies.

DFT Calculations. The ground state geometries of mixed substituted free base porphyrins ($H_2TPP(NO_2)X_6$ and $H_2TPP(NO_2)X_2$) were optimized in the gas phase by DFT calculations using the B3LYP functional and LANL2DZ basis set.[23] Figures 2 and S2–S4, Supporting Information, represent the fully optimized geometries of these porphyrins (top and side views) as well as the deviation of core atoms from the porphyrin mean plane. Selected average bond lengths and bond angles of $H_2TPP(NO_2)X_2$ and $H_2TPP(NO_2)X_6$ are listed in the Tables S3 and S4, Supporting Information, respectively. Observed bond lengths and bond angles in B3LYP/LANL2DZ-optimized geometries of mixed substituted porphyrins are similar to those reported in the literature.[2d,e,22b,c] The nonplanar conformation of free base porphyrins arises by the tilting of the pyrrole rings to prevent repulsive interactions among the substituents, and these result in the increment of bond lengths of $C_\beta-C_\beta$ as well as in the bond angles of $C_\beta-C_\alpha-C_m$ with a concomitant decrease in the bond angles of $N-C_\alpha-C_m$. Herein, $H_2TPP(NO_2)X_2$ systems exhibited about a 2–4° change in these angles, and this change is comparable to that of the saddle-shape $CuTPP(Ph)_4(CH_3)_4$ and H_2TPPTh_4 structures.[21e,24]

Notably, $H_2TPP(NO_2)X_6$ (X = Ph, PE, Br, and Th) exhibited highly nonplanar severe saddle-shape conformational features in comparison to $H_2TPP(NO_2)X_2$. The $C_{\beta'}-C_{\beta'}$ bond lengths (1.391–1.417 Å) of the pyrroles bearing four β-substituents in $H_2TPP(NO_2)X_6$ systems are longer than the $C_\beta-C_\beta$ distances (1.375–1.388 Å) of the antipodal pyrroles bearing three β-substituents (Table S4, Supporting Information). The increment in the bond angles of $C_\beta-C_\alpha-C_m$ with the concomitant decrement in the bond angles of $N-C_\alpha-C_m$ in $H_2TPP(NO_2)X_6$ systems were found to be significantly large (4–8°) in these angles which are comparable to that of H_2TPPX_8 (X = Br, Cl, and Ph)[2d,e] and H_2TPPBr_6 structures.[21c]

dx.doi.org/10.1021/ic501259g | Inorg. Chem. 2014, 53, 12706–12719

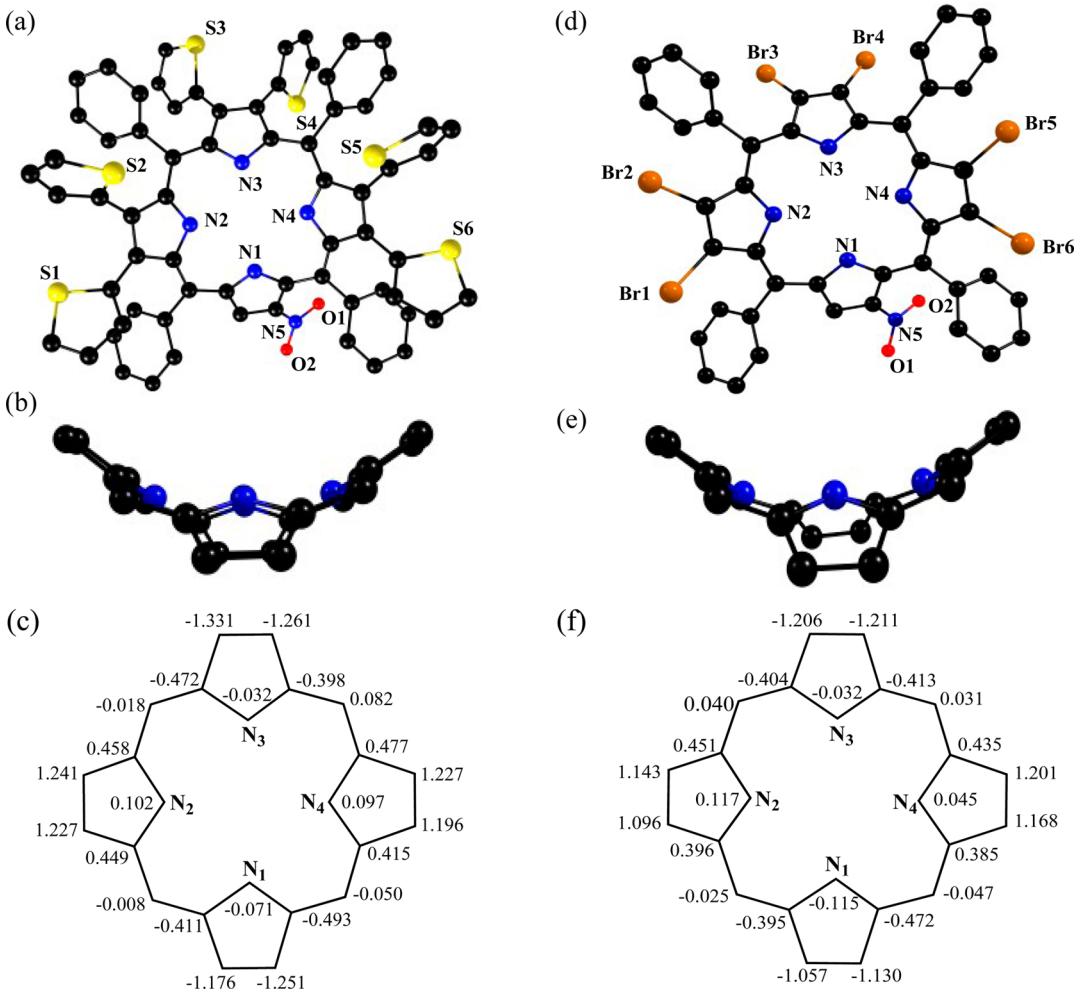

Figure 2. B3LYP/LANL2DZ-optimized geometries showing top as well as side views of $H_2TPP(NO_2)(Th)_6$ (a and b) and $H_2TPP(NO_2)Br_6$ (d and e), respectively. In side view, the *β*-substituents and *meso*-phenyl groups are not shown for clarity. (c and f) Displacement of porphyrin-core atoms (in Angstroms) from the mean plane for $H_2TPP(NO_2)(Th)_6$ and $H_2TPP(NO_2)Br_6$, respectively. Color codes for atoms: C, black; N, blue; O, red; S, yellow; Br, brown.

Table 1. Optical Absorption Spectral Data of Mixed Substituted Porphyrins[a]

porphyrin	B band(s), nm	Q bands, nm
$H_2TPP(NO_2)$	426(5.34)	526(4.21), 604(3.62), 664(3.95)
$H_2TPP(NO_2)Br_2$	436(5.23)	536(4.08), 623(3.43), 683(3.91)
$H_2TPP(NO_2)Ph_2$	439(5.09)	536(4.01), 686(3.80)
$H_2TPP(NO_2)(PE)_2$	444(5.38)	540(4.25), 583(3.99), 687(3.93)
$H_2TPP(NO_2)Th_2$	440(5.24)	540(4.19), 695(4.01)
$H_2TPP(NO_2)(CN)_2$	440(5.47)	541(4.14), 585(4.00), 645(3.79), 702(4.30)
$H_2TPP(NO_2)Br_6$	371(4.39), 468(5.11)	628(3.98), 739(3.80)
$H_2TPP(NO_2)$ Ph_6	377(4.44), 470(5.11)	571(3.83), 624(3.75), 729(3.90)
$H_2TPP(NO_2)(PE)_6$	494(5.22)	586(4.29), 666(sh), 751(3.43)
$H_2TPP(NO_2)Th_6$	325(4.65), 481(4.90)	589(3.61), 644(3.75), 754(3.40)

[a]Values in parentheses refer to log ε (ε in mol^{-1} cm^{-1}).

Among all, $H_2TPP(NO_2)Th_6$ exhibited higher nonplanarity (ΔC_β = ±1.240 Å) as compared to all other porphyrins. The top and side views of $H_2TPP(NO_2)Th_6$ are shown in Figure 2a and 2b, respectively. Figure 2c represents the displacement of porphyrin-core atoms from the mean plane in Angstroms, indicating the severe saddle-shape conformation. The 2-thienyl groups substituted at the *β*-pyrrole carbons are oriented trans to each other in order to minimize the lone pair repulsions as seen in the crystal structures. The mean plane displacement of the *β*-pyrrole carbons (ΔC_β) and the *meso*-carbons from the mean plane follows the order $H_2TPP(NO_2)(CN)_2$ < $H_2TPP(NO_2)(PE)_2$ < $H_2TPP(NO_2)Br_2$ ≈ $H_2TPP(NO_2)Ph_2$ < $H_2TPP(NO_2)(Th)_2$ < $H_2TPP(NO_2)(PE)_6$ < $H_2TPP(NO_2)Br_6$ ≈ $H_2TPP(NO_2)Ph_6$ < $H_2TPP(NO_2)(Th)_6$, indicating the varying degrees of nonplanarity in these mixed substituted porphyrins. The electronic effects of the substituents and the influence of nonplanarity (as evidenced from single-crystal X-ray structures and DFT calculations) on the porphyrin *π*-

dx.doi.org/10.1021/ic501259g | Inorg. Chem. 2014, 53, 12706−12719

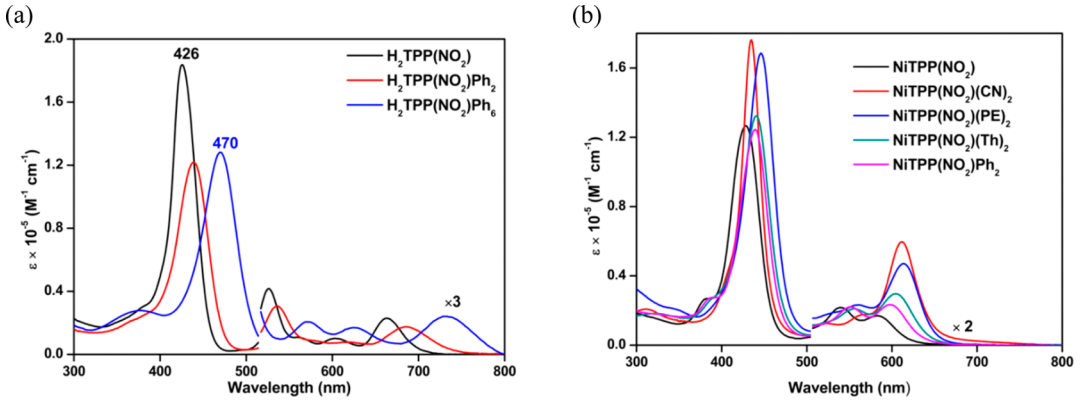

Figure 3. Electronic absorption spectra of (a) $H_2TPP(NO_2)Ph_n$ (n = 0, 2, and 6) and (b) $NiTPP(NO_2)X_2$ (X = H, CN, PE, Th, and Ph) in CH_2Cl_2 at 298 K. Porphyrin concentration was maintained between 7 and 10 μM.

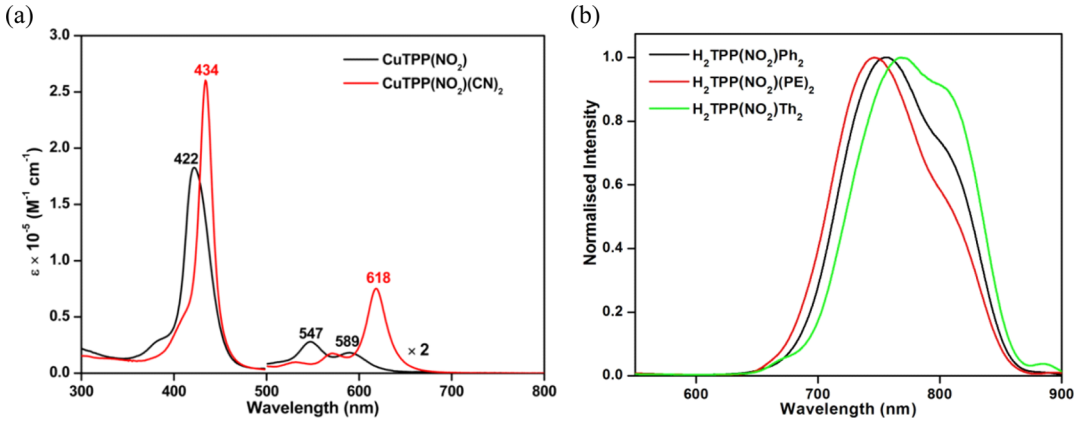

Figure 4. (a) Overlayed optical absorption spectra of $CuTPP(NO_2)$ (8.87 μM) and $CuTPP(NO_2)(CN)_2$ (5.18 μM) in CH_2Cl_2 at 298 K. (b) Fluorescence spectra of $H_2TPP(NO_2)X_2$ (X = Ph, PE, Th) in CH_2Cl_2 at 298 K.

system are further examined by spectroscopic and electrochemical redox studies.

Electronic Spectral Studies. Optical absorption spectra of porphyrins and their metal complexes are influenced by the presence of peripheral substituents and core metal ions.[1,2,10−14,25] It is known that the nonplanar conformation of the macrocycle induces an unusual red shift in their spectral properties.[26,2g] Table 1 lists the absorption spectral data of newly synthesized free base porphyrins in CH_2Cl_2 at 298 K. Representative absorption spectra of $H_2TPP(NO_2)Ph_n$ (n = 0, 2, and 6) and $NiTPP(NO_2)X_2$ are shown in Figure 3a and 3b, respectively. All free base derivatives ($H_2TPP(NO_2)X_n$, where n = 0, 2, 6) exhibited a characteristic Soret band (B band) and three Q bands, whereas H_2TPP shows one B band and four Q bands. $H_2TPP(NO_2)$ exhibited red shifts in the Soret band ($\Delta\lambda_{max}$ = 9 nm) and $Q_x(0,0)$ band ($\Delta\lambda_{max}$ = 17 nm) relative to H_2TPP. $H_2TPP(NO_2)X_2$ (X = Br, Ph, PE, Th, and CN) showed further red shifts in the B band ($\Delta\lambda_{max}$ = 10−20 nm) and $Q_x(0,0)$ band ($\Delta\lambda_{max}$ = 20−30 nm) relative to $H_2TPP(NO_2)$ (Figure S5, Supporting Information). This is possibly due to the inductive and/or conjugative interaction of the substituents with the π-system as well as the nonplanarity of the porphyrin macrocycle as evidenced from the crystal structure of $H_2TPP(NO_2)Th_2$ and the optimized geometries of $H_2TPP(NO_2)X_2$ (vide supra). Table S5, Supporting Information, lists the UV−vis spectral data of all metal complexes. Although the metal complexes, $MTPP(NO_2)X_2$ (M = Co(II), Ni(II), Cu(II), and Zn(II)) bear lower symmetry, they exhibited a B and two Q bands with molar extinction coefficients (ε) similar to those of their corresponding MTPPs (D_{4h}).[27]

$H_2TPP(NO_2)X_6$ (X = Br, Ph, PE, and Th) exhibited large red shifts in the Soret band ($\Delta\lambda_{max}$ = 40−70 nm) and $Q_x(0,0)$ band ($\Delta\lambda_{max}$ = 65−90 nm) relative to $H_2TPP(NO_2)$ due to the increase in the number of X, nonplanarity of the macrocycle, and/or electronic nature of the substituents (Figure S6, Supporting Information). The longest wavelength band ($Q_x(0,0)$) of free-base porphyrins showed an interesting trend in red shift and aligns in the following order: $H_2TPP(NO_2)$ < $H_2TPP(NO_2)Br_2$ < $H_2TPP(NO_2)Ph_2$ < $H_2TPP(NO_2)(PE)_2$ < $H_2TPP(NO_2)(Th)_2$ < $H_2TPP(NO_2)(CN)_2$ < $H_2TPP(NO_2)Ph_6$ < $H_2TPP(NO_2)Br_6$ < $H_2TPP(NO_2)(PE)_6$ < $H_2TPP(NO_2)(Th)_6$. The observed red shift of the $Q_x(0,0)$ band is in accordance with the increment in the number of substituents ($H_2TPP(NO_2)$ < $H_2TPP(NO_2)X_2$ < $H_2TPP(NO_2)X_6$) and the extent of nonplanarity of the porphyrin π-system as evidenced from the crystal structures[21c] and DFT calculations. Further, among the same series ($H_2TPP(NO_2)X_2$ or $H_2TPP(NO_2)X_6$), the electron-withdrawing and/or conjugatively resonating substituents exhibited a large bathochromic shift. Further, mixed substituted $H_2TPP(NO_2)(PE)_6$ showed a dramatic red shift in the B band (68 nm) and $Q_x(0,0)$ band (87 nm) relative to $H_2TPP(NO_2)$. The spectral features of $H_2TPP(NO_2)X_6$ with mixed substituent pattern are similar to those of β-octabromo-[28] or β-octaphenyl-TPPs.[29] The red shift in the highly substituted porphyrins has been ascribed to the nonplanarity of the porphyrin ring in

dx.doi.org/10.1021/ic501259g | Inorg. Chem. 2014, 53, 12706−12719

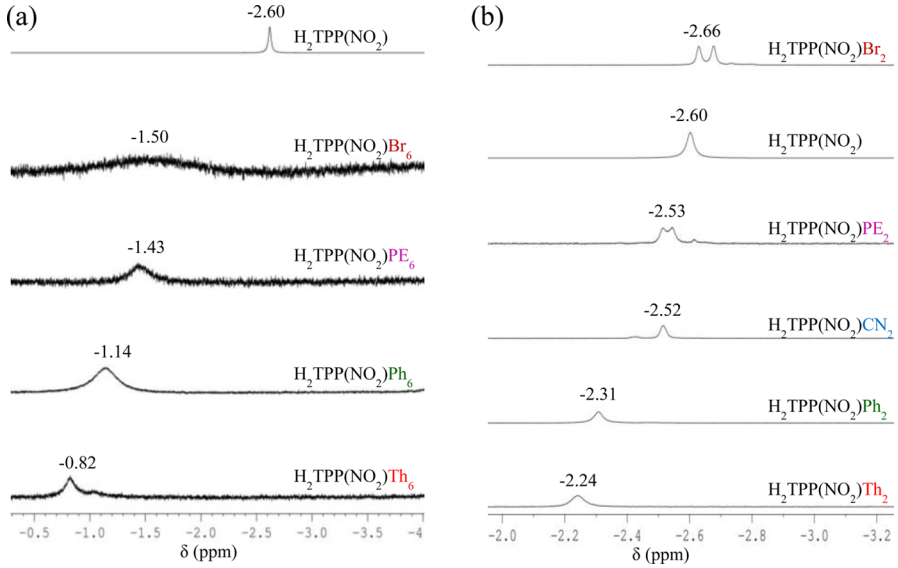

Figure 5. Representative ^{1}H NMR spectra of the imino proton region of (a) $H_2TPP(NO_2)X_6$ (X = Br, PE, Ph, and Th) and (b) $H_2TPP(NO_2)X_2$ (X = Br, PE, Ph, Th, and CN) in $CDCl_3$ at 298 K.

combination with the inductive or conjugative interaction of the substituents that are in direct conjugation with the π-system.

Electronic absorption spectra of representative CuTPP-$(NO_2)X_2$ (X = H, CN) are shown in Figure 4a. Introduction of two more electron-withdrawing groups on the other opposite pyrrole positions of CuTPP(NO_2) showed a bathochromic shift in their spectral features with considerable increment in molar absorptivity (ε). Generally, metal complexes, MTPP$(NO_2)X_2$, exhibited a B band and two Q bands with the extent of red shift of the B band being about 7−20 and 10−30 nm in $Q_x(0,0)$ transitions relative to their corresponding MTPP(NO_2). MTPP$(NO_2)(CN)_2$ complexes showed considerable gain in the intensity of the longest wavelength $Q_x(0,0)$ band relative to the $Q_x(1,0)$ band (Figure 4a), and this is possibly due to stabilization of a_{1u} relative to a_{2u} of MTPP$(NO_2)(CN)_2$, thereby increasing the transition probability of a_{2u} to $e_g(\pi^*)$ relative to a_{1u} to e_g (π^*).[30] MTPP$(NO_2)X_6$ showed a dramatic red shift of 30−70 nm in the Soret band and 35−100 nm in the $Q_x(0,0)$ band as compared MTPP(NO_2). As expected (Table S5), the bands are more blue shifted with the increase in electronegativity of the metal ion.[31] Generally, MTPP$(NO_2)(Ph)_n$ derivatives show blue-shifted absorption spectral features relative to MTPP-$(NO_2)(PE)_n$ or MTPP$(NO_2)(CN)_n$ derivatives. This is possibly due to the variable steric crowding and the electronic nature of the substituent that induces conformational differences between the macrocycles as well as the substituent effects. A pronounced red shift in the absorption spectral features of the mixed substituted cyano, phenylethynyl, and bromoporphyrins is due to push−pull, extended conjugation, and/or nonplanar distortion of the porphyrin ring. The red shift exhibited by nonplanar porphyrins is also supported by theoretical studies.[26]

The synthesized free base and Zn(II) complexes of mixed substituted porphyrins were characterized by fluorescence spectroscopy to elucidate the role of substitution and the effect of nonplanarity. The steady state emission spectra of $H_2TPP(NO_2)X_2$ (X = Ph, PE, and Th) in CH_2Cl_2 is shown in Figure 4b. Table S6, Supporting Information, lists emission data of MTPP$(NO_2)X_n$ in CH_2Cl_2 at 298 K. $H_2TPP(NO_2)X_2$ (X = CN, Ph, PE, and Th) exhibited a more red-shifted emission (75−110 nm) than that of H_2TPP in CH_2Cl_2. Notably, highly red-shifted emission bands ($\Delta\lambda_{max}$ = 160−170 nm) with feeble fluorescence intensity were observed for $H_2TPP(NO_2)X_6$ (X = PE and Th) in comparison to H_2TPP in CH_2Cl_2. The representative emission spectra of MTPP$(NO_2)X_n$ (M = 2H and Zn(II); n = 0, 2, and 6, X = Th, Ph, CN, and PE) are shown in Figures S7−S9, Supporting Information. The free-base porphyrins exhibited an interesting trend in the red shift of their corresponding emission bands and aligns in the following order: H_2TPP < $H_2TPP(NO_2)(CN)_2$ < $H_2TPP(NO_2)(PE)_2$ < $H_2TPP(NO_2)Ph_2$ < $H_2TPP(NO_2)Th_2$ < $H_2TPP(NO_2)(PE)_6$. The increasing order of red shift and the decrement in the quantum yields (Table S6, Supporting Information) are in accordance with the increasing order of nonplanarity of the porphyrin macrocycle as evidenced from X-ray crystallography and DFT calculations. The same trend was also observed for Zn(II) complexes as expected. Notably, $H_2TPP(NO_2)X_6$ (X = Ph, Th, and Br) failed to show emission spectrum due to enhanced nonplanarity which reduces the singlet excited state lifetime in comparison to planar porphyrins as seen in $H_2TPP(Et)_8$ and $H_2TPP(Ph)_8$.[32a−c] Further, quenching of the emission in $H_2TPP(NO_2)Br_2$ and $H_2TPP(NO_2)Br_6$ is ascribed to the combination of nonplanarity and heavy atom effect of bromo groups that are in direct conjugation with the porphyrin π-system. Similar behavior was reported for β-brominated porphyrins, for example, $MTPPBr_4$ exhibited a weak red-shifted emission, while $MTPPBr_8$ failed to show a singlet emission.[28a,32d]

^{1}H NMR Studies. $H_2TPP(NO_2)$ exhibits characteristic chemical shifts arising from the β-pyrrole (9.10−8.71 ppm) and *meso*-phenyl (8.29−7.70 ppm) proton resonances.[9a] ^{1}H NMR spectra of free base mixed substituted porphyrins ($H_2TPP(NO_2)X_n$) (X = Br, Ph, PE, Th, and CN; n = 0, 2, and 6) exhibit resonances arising from *meso*-phenyls, β-pyrrole proton(s), β-substituents (Ph or Th or PE), and imino hydrogens (Figures S10−S29, Supporting Information). The chemical shifts of the *meso*-phenyl protons of $H_2TPP(NO_2)X_n$ are comparable to those observed for the corresponding

dx.doi.org/10.1021/ic501259g | Inorg. Chem. 2014, 53, 12706−12719

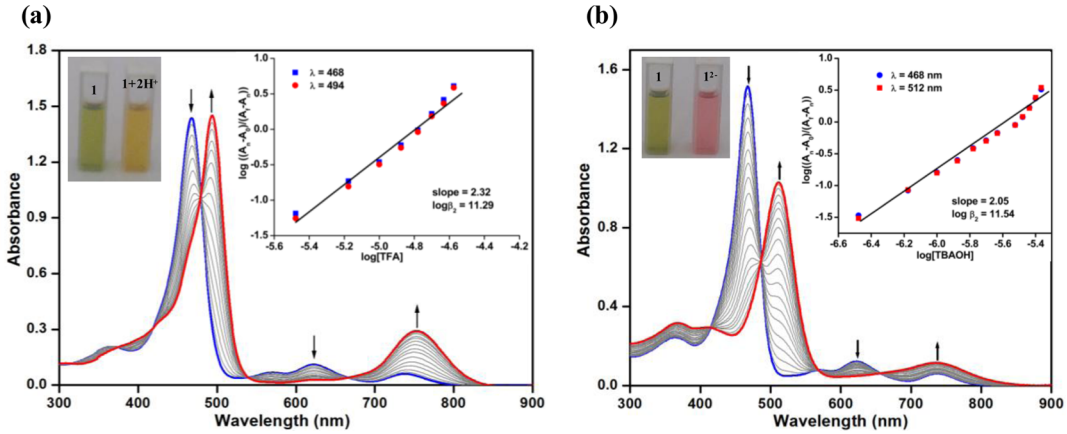

Figure 6. UV−vis spectral titration of $H_2TPP(NO_2)Br_6$ (9×10^{-6} M) with (a) TFA and (b) TBAOH in toluene; (insets) corresponding Hill plots.

$H_2TPP(NO_2)$. The β-pyrrole resonances of $H_2TPP(NO_2)X_2$ (X = Br, Ph, Th, and PE) are marginally upfield shifted (~0.1−0.2 ppm) than that of $H_2TPP(NO_2)$, whereas $H_2TPP(NO_2)(CN)_2$ exhibited a 0.25 ppm downfield shift due to the strong electron-withdrawing nature of cyano groups. The β-pyrrole proton of $H_2TPP(NO_2)X_6$ (X = Br, Ph, PE, and Th) is 0.47−0.80 ppm upfield shifted than $H_2TPP(NO_2)$. The *meso*-phenyl protons of $H_2TPP(NO_2)X_6$ (X = Br, PE, and Th) is marginally shifted in comparison to $H_2TPP(NO_2)$, whereas $H_2TPP(NO_2)Ph_6$ is 0.25−0.41 ppm upfield shifted possibly due to the ring current effect of β-pyrrole phenyl protons. $H_2TPP(NO_2)Ph_6$ exhibited characteristic upfield shifted β-phenyl protons in the range of 6.90−6.47 ppm, which is attributed to the ring current effect of β-pyrrole phenyl protons, whereas β-phenylethynyl protons resonate between 7.18 and 7.36 ppm, indicating phenyl protons are distant from the ring current. The core imino protons, β-pyrrole protons, and β-thienyl C-3 protons of H_2TPPTh_n (n = 2 and 6) resonating at the downfield region are possibly due to the inductive effect of 2-thienyl groups, which leads to decrement in the ring current of the porphyrin π-system.[24b]

Figure 5 shows the ^{1}H NMR spectra of the imino proton region of $H_2TPP(NO_2)X_6$ and $H_2TPP(NO_2)X_2$ in $CDCl_3$ at 298 K. The core imino protons of $H_2TPP(NO_2)Br_6$ (−1.5 ppm), $H_2TPP(NO_2)(PE)_6$ (−1.43 ppm), $H_2TPP(NO_2)Ph_6$ (−1.14 ppm), and $H_2TPP(NO_2)(Th)_6$ (−0.82 ppm) are downfield shifted relative to $H_2TPP(NO_2)$ (−2.60 ppm) as shown in Figure 5a. The imino proton resonances of the $H_2TPP(NO_2)X_2$ series, $H_2TPP(NO_2)(PE)_2$ (−2.53 ppm), $H_2TPP(NO_2)(CN)_2$ (−2.52 ppm), $H_2TPP(NO_2)Ph_2$ (−2.31 ppm), and $H_2TPP(NO_2)(Th)_2$ (−2.24 ppm) are more downfield shifted than $H_2TPP(NO_2)$, whereas $H_2TPP(NO_2)Br_2$ (−2.65 ppm) is slightly upfield shifted (Figure 5b). Further, the downfield shift of the resonances is due to substituent effects and/or the nonplanar conformation as observed in the X-ray crystal structures and optimized geometries. Nonplanarity of the macrocycle causes the broad features of the imino protons to resonate at the downfield region relative to that in planar porphyrins (Figure 5a).[33] The reason for the largest downfield shift of NH protons of $H_2TPP(NO_2)(Th)_6$ is enhanced nonplanarity and an inductive effect induced by thienyl groups which leads to decrement in the ring current of the macrocycle.[24b]

^{1}H NMR spectra of $MTPP(NO_2)X_n$ (M = Zn(II) and Ni(II); n = 2 and 6) complexes are devoid of imino protons, revealing that metal ion got inserted into the porphyrin ring. The β-proton resonances for $NiTPP(NO_2)X_n$ are marginally upfield shifted (0.03−0.11 ppm), whereas in the case of $ZnTPP(NO_2)X_n$ they are marginally downfield shifted (0.02−0.26 ppm) in comparison to their corresponding $H_2TPP(NO_2)X_n$ derivatives. The *meso*-phenyl protons resonances of $MTPP(NO_2)X_n$ are marginally upfield (0.05−0.43 ppm) corresponding to those of free base derivatives. The integrated intensities of the proton resonances of these mixed substituted porphyrins are consistent with the proposed structures.

Protonation and Deprotonation Studies. To examine the effect of mixed substitution on nonplanarity, we carried out protonation and deprotonation studies in toluene using trifluoroacetic acid (TFA) and tetrabutylammonium hydroxide (TBAOH), respectively. Figure 6 shows the UV−vis spectral changes of $H_2TPP(NO_2)Br_6$ while increasing the concentration of TFA ($0.33–6.29 \times 10^{-5}$ M) and TBAOH ($0.33–6.62 \times 10^{-6}$ M). Table 2 lists the protonation and deprotonation constants of various free base mixed substituted porphyrins. Figure 6a shows the concomitant decrement in absorbance of $H_2TPP(NO_2)Br_6$ at 468 nm and rising of a new band at 494 nm while increasing the concentration of TFA. As protonation proceeds, the multiple Q bands are disappearing and a new single broad band grows at 753 nm accompanied by the red shift of 16 nm in the $Q_x(0,0)$ band. In all cases, we could obtain diprotonated porphyrin species which is further confirmed by a Hill plot having a slope of ~2 as shown in Figures 6a, inset, and

Table 2. Protonation and Deprotonation Constants of Free Base Mixed Substituted Porphyrins in Toluene at 298 K

	TFA			TBAOH		
porphyrin	$\log \beta_2$	slope	r^2	$\log \beta_2$	slope	r^2
$H_2TPP(NO_2)Br_6$	11.29	2.32	0.93	11.54	2.05	0.94
$H_2TPP(NO_2)Ph_6$	11.74	1.99	0.88			
$H_2TPP(NO_2)Th_6$	11.21	2.12	0.84	7.91	1.65	0.80
$H_2TPP(NO_2)PE_6$	8.47	2.01	0.85	11.34	2.36	0.97
H_2TPPBr_8	10.53	2.10	0.97	10.40	2.00	0.91
H_2TPPCl_8	9.21	2.01	0.99	10.21	1.90	0.96
$H_2TPP(NO_2)Br_2$	7.92	2.50	0.98			
$H_2TPP(NO_2)Ph_2$	9.54	1.91	0.98			
$H_2TPP(NO_2)Th_2$	8.76	1.95	0.97			
$H_2TPP(NO_2)PE_2$	8.65	2.64	0.99			
$H_2TPP(NO_2)CN_2$	3.69	2.18	0.93			

dx.doi.org/10.1021/ic501259g | Inorg. Chem. 2014, 53, 12706−12719

S30, Supporting Information, and Table 2. All diprotonated species of mixed substituted porphyrins are stable and showing aromatic nature as evidenced by the UV−vis spectral features. $H_2TPP(NO_2)X_6$ (X = Br, Ph, and Th) exhibits ∼6−288-fold higher protonation constants (β_2) in comparison to H_2TPPX_8 (X = Br, Cl) in toluene, which is ascribed to the combined effect of mixed substitution and nonplanarity. The observed log β_2 values of H_2TPPX_8 (X = Br, Cl) in toluene are comparable to those observed in CH_2Cl_2.[21h]

$H_2TPP(NO_2)(PE)_6$ has shown a (∼5.52−18.6 × 10^2)-fold lower β_2 value which is ascribed to the electron-withdrawing nature of the phenylethynyl groups and less nonplanar conformation as compared to $H_2TPP(NO_2)X_6$ (X = Br, Ph, and Th). $H_2TPP(NO_2)(CN)_2$ exhibited a much lower log β_2 value (3.69) than that of $H_2TPP(NO_2)X_2$ (X = Br, Ph, PE, and Th), which is attributed to the combined effect of the quasi-planar structure (ΔC_β = ±0.5 Å and over all mean plane deviation of porphyrin core, Δ24 = 0.234 Å) and strong electron-withdrawing nature of the cyano and nitro substituents. $H_2TPP(NO_2)X_2$ (X = Br, Ph, PE, and Th) were shown to have lower log β_2 values (7.9−9.54) in comparison to H_2TPPR_4 (R = Me, Ph, Th, and Br) with log β_2 values (9.03−9.96)[21h] possibly due to the strong electron-accepting nature of the nitro group. Figure 6b shows the concomitant decrement in the absorbance of $H_2TPP(NO_2)Br_6$ at 468 nm while increasing the concentration of TBAOH, and a new band rises at 512 nm. As deprotonation proceeds the multiple Q bands of the neutral compound disappear and a new band rises at 736 nm. The inset shows the Hill plot with a slope of ∼2 and log β_2 value of 11.54 which reveals the acidic nature of the NH protons due to the electron-withdrawing nature of NO_2 and Br substituents. Notably, $H_2TPP(NO_2)(PE)_6$ has a close log β_2 value to $H_2TPP(NO_2)Br_6$, reflecting the electron-accepting nature of the substituents (nitro and phenylethynyl groups) and induced nonplanarity by mixed substitution. Further, $H_2TPP(NO_2)Th_6$ has a lower deprotonation constant as compared to $H_2TPP(NO_2)(PE)_6$ and $H_2TPP(NO_2)Br_6$, which is interpreted in terms of the conjugative effect of the 2-thienyl groups.[24b] Under similar conditions, $H_2TPP(NO_2)Ph_6$ was showing incomplete deprotonation with split Soret bands (Figure S31c, Supporting Information) even at a higher concentration of the base. This is possibly due to the electron-rich nature of the porphyrin core which prevents formation of dianionic species. Moreover, at very high concentrations of TBAOH, the reactant is in equilibrium with the anionic species and does not move forward to completion. $H_2TPP(NO_2)X_2$ (X = Br, Ph, PE, Th, and CN) does not show any spectral changes upon addition of very high concentration of TBAOH (5.97 × 10^{-4} M), which indicates the moderate nonplanar conformation (ΔC_β = ±0.67−0.73 Å) of the porphyrin π-system as compared to $H_2TPP(NO_2)X_6$ (ΔC_β = ±1.01−1.24 Å).

Electrochemistry. The redox potentials of the porphyrin π-system are influenced by the nonplanar conformation, nature of the substituents, and core metal ions. To determine the influence of macrocyclic nonplanarity and the combined effects of electron-donor and -acceptor groups at the β-pyrrole positions, we examined the electrochemical redox properties of these mixed substituted porphyrins by cyclic voltammetric studies. Under similar conditions, the corresponding $MTPP(NO_2)$ and MTPP[21e] derivatives were also examined, and the electrochemical redox data (vs Ag/AgCl) are listed in Table 3.

The influence of different β-substituents on the redox potentials for $CuTPP(NO_2)X_2$ and $CuTPP(NO_2)X_6$ are shown in Figure 7. Table S7, Supporting Information, lists the electrochemical redox data (vs Ag/AgCl) of various metal complexes in CH_2Cl_2 at 298 K. The mixed substituted porphyrins exhibited two successive one-electron electrochemical oxidations and reductions, whereas Co(II) complexes show first metal-centered redox behavior followed by a π-system. Generally, the first oxidation of Co(II) porphyrins is a metal-centered process and well documented in the literature.[10c,34a,b] Further, we carried out the oxidation of Co(II) porphyrins to Co(III) porphyrins by adding aliquots of *tert*-butyl hydroperoxide (TBHP) in CH_2Cl_2 as chemical oxidant which is reflected in the UV−vis spectral changes as shown in the Supporting Information (Figure S32 and Table S8). The effect of mixed β-substitution (tri and hepta) as well as the effect of core metal ion on redox potentials of $MTPP(NO_2)X_n$ (n = 0, 2 and 6; X = Br, CN, PE, Ph and Th; M = 2H, Co(II), Ni(II), Cu(II) and Zn(II)) are shown in Figures S33−S36, Supporting Information.

Table 3. Electrochemical Redox Potentials (in V vs Ag/AgCl) of Mixed Substituted Porphyrins in CH_2Cl_2 Containing 0.1 M $TBAPF_6$ with a Scan Rate of 0.1 V/s at 298 K

	oxidation (mV)		reduction (mV)		ΔE (mV)
porphyrin	I	II	I	II	
H_2TPP	1000	1335	−1230	−1540	2230
$H_2TPP(NO_2)$	1100	1286	−874	−1086	1974
$H_2TPP(NO_2)Br_2$	1118	1214	−754	−824	1872
$H_2TPP(NO_2)Ph_2$	1009	1130	−849	−1028	1858
$H_2TPP(NO_2)(PE)_2$	1123	1233	−752	−827	1875
$H_2TPP(NO_2)Th_2$	1007	1132	−800	−925	1807
$H_2TPP(NO_2)(CN)_2$	1294	1462	−519	−827	1813
$H_2TPP(NO_2)Br_6$	1045[a]	1288[a]	−642[a]	−973[a]	1687
$H_2TPP(NO_2)Ph_6$	804[a]	1091[a]	−921[a]	−1354[a]	1725
$H_2TPP(NO_2)(PE)_6$	1098[a]	1185[a]	−659	−732	1757
$H_2TPP(NO_2)Th_6$	806[a]	1033	−805	−1345	1611

[a]Refers to irreversible peak potential.

The first ring oxidation potentials for $MTPP(NO_2)X_2$ (X = Br, Ph, PE, Th, and CN and M = 2H, Co(II), Ni(II), Cu(II), and Zn(II)) span a range from 0.85 to 1.33 V, whereas the reduction potential varies from −0.63 to −1.07 V (Tables 3 and S7, Supporting Information). The first ring redox potentials of $MTPP(NO_2)(CN)_2$ have a 200−350 mV anodic shift in comparison to $MTPP(NO_2)Ph_2$, which is attributed to the strong electron-withdrawing nature of the cyano substituents. The metal-centered reduction potential of $CoTPP(NO_2)(CN)_2$ is 470 mV anodically shifted as compared to CoTPP due to the strong electron-withdrawing nature of nitro and cyano groups. The metal-centered redox potentials are altered according to the electronic nature of the substituents rather than the influence of nonplanarity. Notably, trimixed substituted porphyrins show the following trend in their first oxidation potentials: $MTPP(NO_2)Ph_2 \leq MTPP(NO_2)Th_2 < MTPP(NO_2) < MTPP(NO_2)(PE)_2 < MTPP(NO_2)Br_2 < MTPP(NO_2)(CN)_2$. This trend is in accordance with the electronic nature of the substituents. The cathodic shift in the oxidation potentials of $MTPP(NO_2)Ph_2$ relative to $MTPP(NO_2)$ is explained in terms of the electron-donating nature of the phenyl groups. For the Hammett equation $E_{1/2} = 2\sigma\rho$ for $MTPP(NO_2)X_2$, the plot of the first ring oxidation and reduction vs the Hammett parameter (σ_p) of the substituents

dx.doi.org/10.1021/ic501259g | Inorg. Chem. 2014, 53, 12706−12719

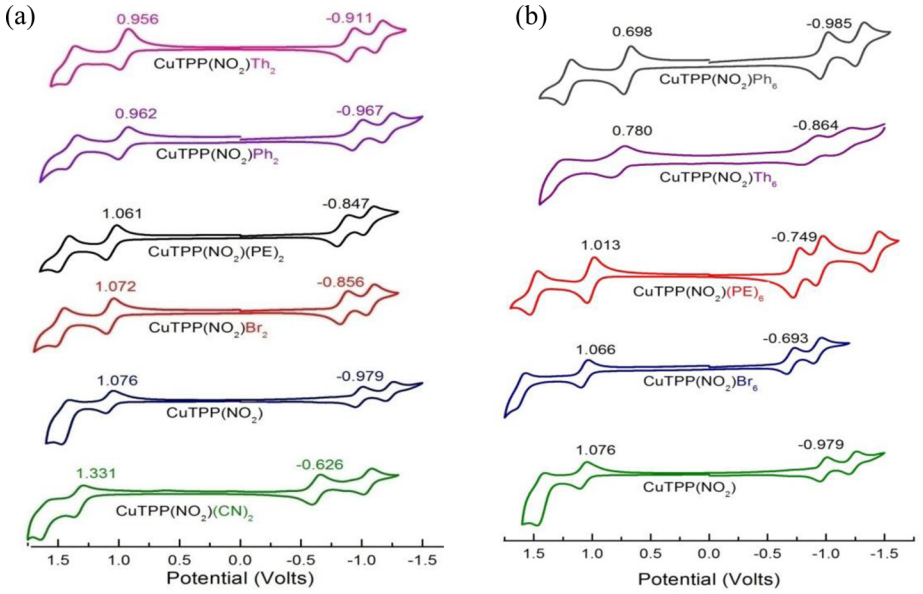

Figure 7. Cyclic voltammograms of (a) $CuTPP(NO_2)X_2$ (~1 mM) and (b) $CuTPP(NO_2)X_6$ (~1 mM) in CH_2Cl_2 containing 0.1 M $TBAPF_6$ using Ag/AgCl as reference electrode with a scan rate of 0.10 V/s at 298 K.

(X)[35] in $MTPP(NO_2)X_2$ was examined to delineate the role of X on the redox potentials, and they show a more linear trend in reduction and oxidation (Figure S38, Supporting Information, and Table 4). The reaction constant (ρ) for oxidation of

Table 4. Summary of Hammett Plots with Reaction Constants (ρ) and Correlation Coefficients (r^2) of First Ring Redox Potentials (vs Ag/AgCl) for Various Mixed Substituted Porphyrins[a]

	first oxidation		first reduction	
porphyrin	ρ (V)	r^2	ρ (V)	r^2
$H_2TPP(NO_2)X_2$	0.193	0.86	0.249	0.98
$CuTPP(NO_2)X_2$	0.251	0.86	0.252	0.98
$NiTPP(NO_2)X_2$	0.121	0.77	0.154	0.87
$ZnTPP(NO_2)X_2$	0.146	0.92	0.261	0.99
$H_2TPP(NO_2)X_6$	0.117	0.23	0.194	0.95
$CuTPP(NO_2)X_6$	0.154	0.31	0.206	0.97
$NiTPP(NO_2)X_6$	0.187	0.62	0.232	0.97
$ZnTPP(NO_2)X_6$	0.117	0.42	0.161	0.88

[a] $MTPP(NO_2)X_n$, where X = Br, CN, Ph, PE, and Th.

$MTPP(NO_2)X_2$ is in the range 0.12−0.25 V, whereas for the reduction it ranges from 0.12 to 0.19 V. The effects of trisubstitution in $CuTPP(NO_2)X_2$ on redox potentials and the HOMO−LUMO gap is shown in Figure S37, Supporting Information. Almost the same trend was observed for $H_2TPP(NO_2)X_2$ and other metal complexes (Table 4). In the $MTPP(NO_2)X_2$ series, the first ring redox potentials varied according to the electronic nature of the substituents with marginal modulation in the HOMO−LUMO gap (~0.2 V as compared to $MTPP(NO_2)$), which is in accordance with the observed moderate nonplanar conformation of the $MTPP(NO_2)X_2$ series (vide supra).

Further, we carried out electrochemical studies of $MTPP(NO_2)X_6$ in order to examine the effect of the number of substituents and nonplanarity (Figures S34−S36, Supporting Information). The first ring oxidation potentials of these porphyrins ranges from 0.68 to 1.31 V, whereas the reduction potential varies from −0.69 to −1.08 V, which shows the broader range in comparison to $MTPP(NO_2)X_2$. The metal-centered reduction potentials of $CoTPP(NO_2)X_6$ is 0.2−0.6 V more anodically shifted than CoTPP, whereas oxidation potentials are less shifted (0.04−0.2 V). This indicates that the electron-withdrawing groups influence significantly the metal-centered reduction rather than oxidation. For the Hammett equation $E_{1/2} = 6\sigma\rho$ for $MTPP(NO_2)X_6$, the Hammett plots were constructed to delineate the role of X on the potentials, and they show a linear trend in reduction, whereas more scattered points in oxidation were observed with poor r^2 values (Figure S38, Supporting Information, and Table 4). The scattered points of oxidation in the Hammett plot indicates the nonplanar confirmation of macrocycle as evidenced from DFT calculations. This is further supported by downfield resonances of NH signals of $H_2TPP(NO_2)X_6$ in ^1H NMR spectroscopy. Figure 8 shows the cyclic voltammograms of $CuTPP(NO_2)X_n$ (X = Ph or Th; n = 0, 2, 6) bearing β-pyrrole phenyl or thienyl substituents. The oxidation potentials of $CuTPP(NO_2)Ph_6$ is ~0.38 V cathodically shifted in comparison to $CuTPP(NO_2)$, whereas reduction is almost unaltered, indicating that each phenyl groups shifts 60 mV cathodic (Figure 8) due to the electron-donating nature of the Ph groups and increased nonplanarity. Notably, $CuTPP(NO_2)Th_6$ exhibited a 0.3 V cathodic shift in oxidation relative to $CuTPP(NO_2)$, whereas a 0.12 V anodic shift in reduction was observed. The observed cathodic shift in oxidation is ascribed to the combined effect of the electron-releasing conjugative nature of 2-thienyl groups and the highly nonplanar conformation of the macrocycle, whereas an anodic shift in reduction is due to the electron-withdrawing inductive effect of the 2-thienyl groups.[24b]

Notably, the first oxidation potentials of $MTPP(NO_2)X_6$ (X = Ph and Th) are more cathodically shifted (0.15−0.25 V), while the reduction potentials are marginally cathodic (0.03−0.06 V) relative to their corresponding $MTPP(NO_2)X_2$ derivatives due to the nonplanar conformation of the macrocycle which destabilizes the HOMO. The ρ value (reactivity constant) for oxidation of $MTPP(NO_2)X_6$ is in the

dx.doi.org/10.1021/ic501259g | Inorg. Chem. 2014, 53, 12706−12719

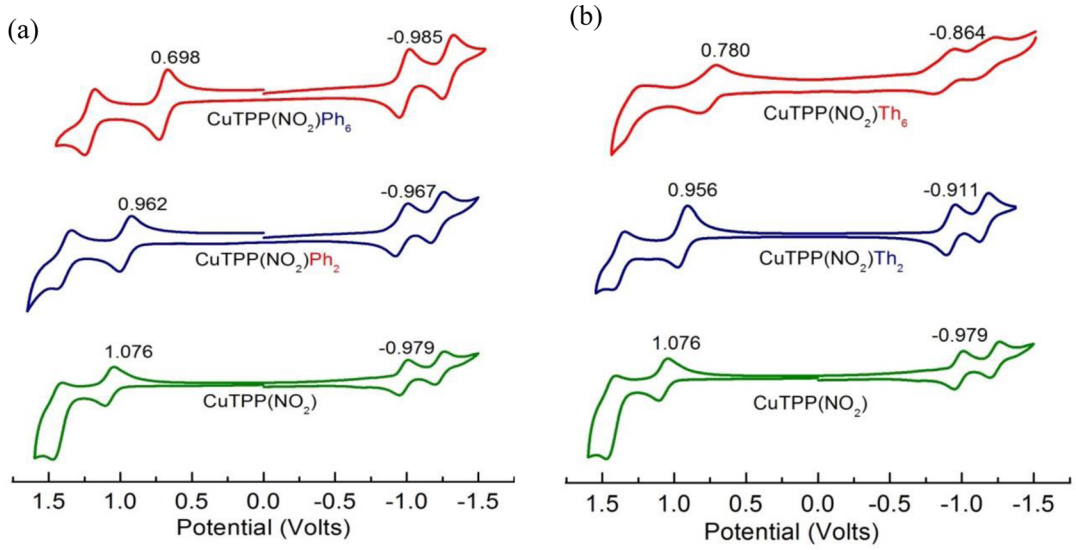

Figure 8. Cyclic voltammograms of (a) CuTPP(NO_2)Ph_n and (b) CuTPP(NO_2)Th_n (n = 0, 2, and 6) in CH_2Cl_2 containing 0.1 M $TBAPF_6$ using Ag/AgCl as reference electrode with a scan rate of 0.1 V/s at 298 K. Porphyrin concentration was maintained ∼1 mM.

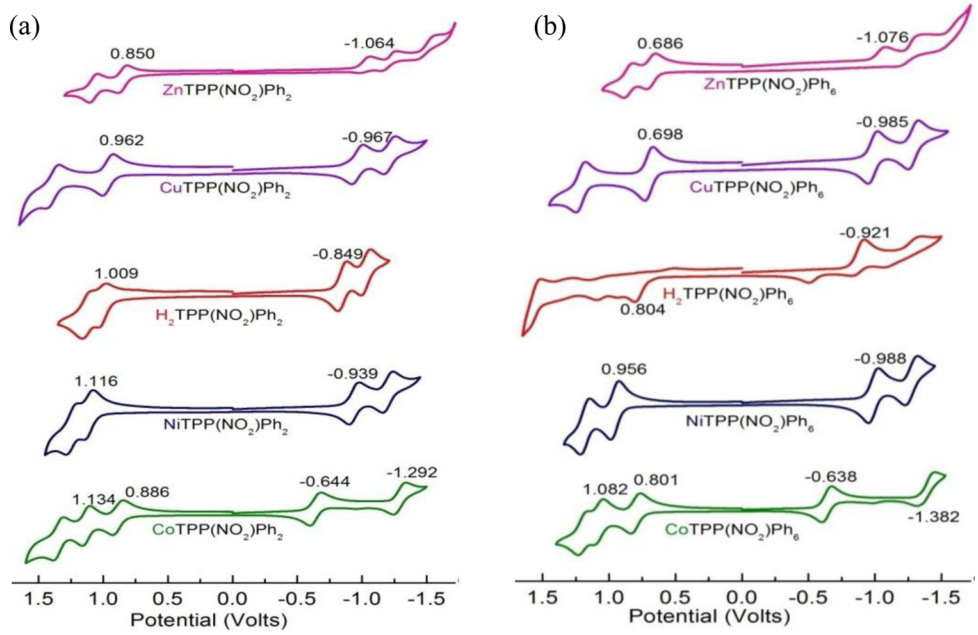

Figure 9. Cyclic voltammograms of (a) MTPP(NO_2)Ph_2 and (b) MTPP(NO_2)Ph_6 (M = 2H, Co(II), Ni(II), Cu(II), Zn(II)) in CH_2Cl_2 containing 0.1 M $TBAPF_6$ using Ag/AgCl as reference electrode at 298 K.

range of 0.15−0.26 V, whereas for the reduction it ranges from 0.16 to 0.21 V. The higher ρ values for oxidation of MTPP(NO_2)X_6 as compared to MTPP(NO_2)X_2 systems indicate the ease of oxidations due to enhanced nonplanarity of the macrocycle. β-Substituted TPP series, viz. MTPP(NO_2)-X_2, MTPP(NO_2)X_6, MTPPX_n (n = 1, 4),[9b,24a,34c,d] exhibited ρ values higher than that reported for the β-octabromo/chloro MT(4-X-phenyl)P (ρ = 0.03−0.08 V)[36] and MT(4-X-phenyl)P series (ρ = 0.065 V).[37] This is anticipated since substitution at the β-pyrrole position is in direct conjugation with the porphyrin π-system, so that higher ρ values were observed.

The effect of the core metal ion on the redox potentials of the representative porphyrins MTPP(NO_2)Ph_n (n = 2 and 6; M = Co(II), Ni(II), Cu(II), and Zn(II)) is shown in Figure 9. The first ring oxidation potentials of these porphyrins show the following trend Zn(II) < Cu(II) < H_2 < Ni(II) < Co(II) for both tri- and heptasubstituted porphyrins according to the difference in their electronegativity. In MTPP(NO_2)X_6 series, the first ring redox potentials varied significantly according to the electronic nature of the substituents and enhanced nonplanarity upon substitution which results in the dramatic reduction in the HOMO−LUMO gap (0.54−0.66 V) as referenced from MTPP (Figure 10). By means of unsymmetrical substitution, we are able to tune the redox potentials with dramatic decrement in the HOMO−LUMO gap. The fairly broader range of σ values for the first ring redox potentials of mixed substituted porphyrins is possibly due to the effect of the core metal ion and the nature of the mixed substituents at the β-pyrrole positions. As reported earlier, the oxidation potentials are largely influenced by the substituent effect and

dx.doi.org/10.1021/ic501259g | Inorg. Chem. 2014, 53, 12706−12719

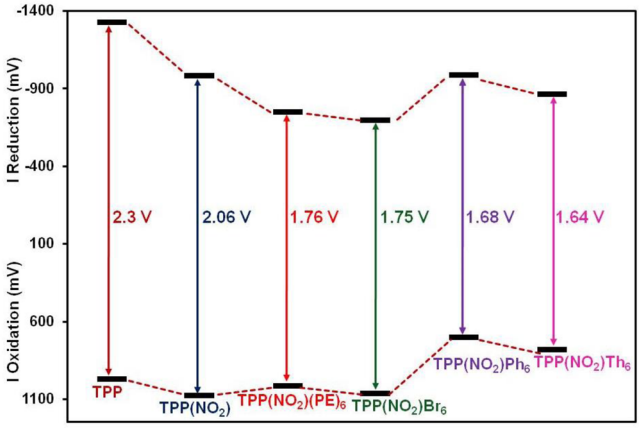

Figure 10. HOMO−LUMO variation of $CuTPP(NO_2)X_6$, where X = PE, Br, Ph, and Th, in comparison to $CuTPP(NO_2)$ and CuTPP.

nonplanarity of the porphyrin macrocycle while the reduction potentials are independent of structural change.[18,38] The almost planar structure of H_2TPPBr_2[21c] is anticipated to show variable degrees of nonplanarity with an increase in size or shape of the substituent X in $MTPP(NO_2)X_6$ derivatives. The crystal structure of H_2TPPBr_6 showed a considerable nonplanar conformation of the porphyrin ring.[21c] The ease of oxidation in $MTPP(NO_2)X_6$ relative to the corresponding $MTPP(NO_2)X_2$ derivatives is ascribed to the electronic effects of the substituents and nonplanar distortion of the macrocycle; however, the reduction potentials are predominantly dependent on the nature of the substituents.

The electrochemical redox potentials and UV−vis spectral data of these unsymmetrically substituted free base porphyrins were compared with the literature having symmetrical β-pyrrole substituents H_2TPPX_4 (X = Br, Ph, Th, and CN) and H_2TPPX_8 (X = Br, PE and Ph) derivatives as shown in Table 5. $\Delta E_{1/2}$ from the redox potentials correlates fairly well with the HOMO−LUMO gap calculated from the longest wavelength band in the optical absorption spectra of these mixed substituted porphyrins. $Q_x(0,0)$ and $\Delta E_{1/2}$ of mixed tri- and heptasubstituted porphyrins are of comparable energy relative to β-tetra- and octasubstituted porphyrins (H_2TPPX_n, n = 4 and 8) as indicated in Table 5. These results clearly indicate that the tri- and heptamixed substitution can compensate for the effect of homo tetra- and octasubstituted porphyrins.

Table 5. Comparison of First Ring Redox Data ($\Delta E_{1/2}$) with Longest Wavelength Band Energy $Q_x(0,0)$ of Various Porphyrins in CH_2Cl_2 at 298 K

porphyrin	B (nm)	$Q_x(0,0)$ (nm)	$Q_x(0,0)$ (eV)	$\Delta E_{1/2}$ (V)[b]	ref
$TPP(NO_2)(PE)_2$	444	687	1.80	1.87	*a*
$TPP(NO_2)Ph_2$	439	686	1.80	1.85	*a*
$TPP(NO_2)Br_2$	436	683	1.82	1.87	*a*
$TPP(NO_2)Th_2$	440	695	1.78	1.80	*a*
$TPP(NO_2)(CN)_2$	440	702	1.77	1.81	*a*
$TPP(PE)_4$	452	690	1.80	1.90	*a*
$TPPPh_4$	434	677	1.83	2.02	39a
$TPPBr_4$	436	685	1.81	1.84	40a
$TPPTh_4$	445	701	1.77	1.94	24b
$TPP(CN)_4$	449	729	1.70	1.66	9b
$TPP(NO_2)(PE)_6$	494	751	1.65	1.75	*a*
$TPP(NO_2)Ph_6$	470	729	1.70	1.72	*a*
$TPP(NO_2)Br_6$	468	739	1.67	1.68	*a*
$TPP(NO_2)Th_6$	481	754	1.64	1.61	*a*
$TPP(PE)_8$	506	761	1.63	1.71	39b
$TPPPh_8$	468	724	1.71	1.84	40b
$TPPBr_8$	469	743	1.67	1.64	28a
TPP	414	646	1.92	2.23	16f

[a]Refers this work. [b]$\Delta E_{1/2} = I_{oxidation} - I_{reduction}$.

CONCLUSIONS

Two new families of novel mixed substituted porphyrins and their metal complexes have been synthesized and characterized. Crystal structure analyses and DFT fully optimized geometries of $MTPP(NO_2)X_2$ and $MTPP(NO_2)X_6$ revealed moderate and highly nonplanar saddle-shape conformations, respectively. These unsymmetrically substituted porphyrins exhibited a dramatic red shift in their B and $Q_x(0,0)$ bands as compared to $MTPP(NO_2)$ and MTPP. The dramatic downfield shift of the NH proton resonances and the higher protonation/deprotonation constants of $H_2TPP(NO_2)X_6$ readily reflects the electronic effects of the mixed substituents (X) and nonplanarity of the macrocycle as compared to $H_2TPP(NO_2)X_2$. The fairly broad range of the first ring redox potentials (from 0.68 to 1.31 V for oxidation and from −0.64 to −1.10 V for reduction) and σ values of $MTPP(NO_2)X_6$ clearly indicate the redox tunability achieved by means of unsymmetrical substitution. Further, the HOMO−LUMO gap considerably decreases as we increase the number of β-substituents from 3 to 7, i.e., $MTPP(NO_2)X_2$ to $MTPP(NO_2)X_6$. The remarkable red shift in electronic spectral features, downfield shift of NH protons, variation in protonation and deprotonation constants, and significant shift in redox potentials of these porphyrins are interpreted in terms of both inductive and resonance interactions of substituents on the porphyrin π-system as well as nonplanarity of the macrocycle. $\Delta E_{1/2}$ obtained from the redox potentials as well as from spectral data ($Q_x(0,0)$ band) suggests that the unsymmetrical tri- and heptasubstitution can compensate for the effect of homo tetra- and octasubstitution of porphyrins (H_2TPPX_n, n = 4 and 8). By means of β-pyrrole mixed substitution on the porphyrin macrocycle we were able to achieve the remarkable bathochromic shift in electronic spectral bands, varying degrees of nonplanarity, higher reactivity constants (ρ values), and tunable electrochemical redox properties with a dramatic reduction in the HOMO−LUMO gap. Currently, we are utilizing these mixed substituted porphyrins for nonlinear optical studies, catalytic, and sensor applications and will report on these studies in the near future.

ASSOCIATED CONTENT

Supporting Information

Experimental section containing synthetic procedures, figures of optical absorption and emission spectra, ^1H NMR spectra, UV−vis titrations for protonation and deprotonation, cyclic voltammetric studies, and XRD data of novel mixed substituted porphyrins. This material is available free of charge via the Internet at http://pubs.acs.org.

AUTHOR INFORMATION

Corresponding Author

*E-mail: sankafcy@iitr.ac.in.

Notes

The authors declare no competing financial interest.

■ ACKNOWLEDGMENTS

We are grateful for the financial support provided by the Council of Scientific and Industrial Research (01(2694)/12/EMR-II), Science and Engineering Research Board (SB/FT/CS-015/2012), and Board of Research in Nuclear Science (2012/37C/61/BRNS). We sincerely thank the reviewers for their valuable suggestions to improve the manuscript. We thank Ms. Neetu Singh and Prof. U. P. Singh, IIT Roorkee, for single-crystal X-ray data collection, and Ms. Pinky Yadav, IIT Roorkee, for DFT calculations. We are thankful to Dr. Koya Prabhakara Rao, VFSTR University, and Dr. P. Ramesh, Samsung Biomedical Research Institute, for suggestions related to X-ray structure solutions. R.K. thanks the Ministry of Human Resource Development (MHRD), India, for the fellowship.

■ REFERENCES

(1) (a) Hoffman, B. M. In *The Porphyrins*; Dolphin, D., Ed.; Academic Press: San Diego, 1979; Vol. *VII*, pp 403−472. (b) Mcdermott, G. S.; Prince, M.; Freer, A. A.; Hawthornthwaite-Lawless, A. M.; Papiz, M. Z.; Cogdell, R. J.; Isaacs, N. W. *Nature* **1995**, *374*, 517−521. (c) Glusker, J. P. In *Vitamin B12*; Dolphin, D., Ed.; John Wiley and Sons: New York, 1982; Vol. *1*, pp 23−106. (d) Summers, J. S.; Petersen, J. L.; Stolzenberg, A. M. *J. Am. Chem. Soc.* **1994**, *116*, 7189−7195. (e) *The Bioinorganic Chemistry of Nickel*; Lancaster, J. R., Ed.; VCH Publishers: New York, 1988; pp 141−165. (f) Qiu, D.; Kumar, M.; Ragsdale, S. W.; Spiro, T. G. *Science* **1994**, *264*, 817−819. (g) *Cytochrome P-450: Structure, Mechanism, and Biochemistry*; Oritz de Montellano, P. R., Ed.; Plenum Press: New York, 1986; pp 1−652. (h) Grinstaff, M. W.; Hill, M. G.; Labinger, J. A.; Gray, H. B. *Science* **1994**, *264*, 1311−1313.

(2) (a) Morgan, B.; Dolphin, D. *Struct. Bonding (Berlin)* **1987**, *64*, 115−187. (b) Ravikanth, M.; Chandrashekar, T. K. *Struct. Bonding (Berlin)* **1995**, *82*, 1−83. (c) Shelnutt, J. A.; Song, X.-Z.; Ma, J.-G; Jia, S.-L.; Jentzen, W.; Medforth, C. J. *Chem. Soc. Rev.* **1998**, *27*, 31−42. (d) Senge, M. O. *The Porphyrin Handbook*; Kadish, K. M., Smith, K. M., Guilard, R., Eds.; Academic Press: San Diego, 2000; Vol. *1*, pp 239−347. (e) Senge, M. O. *Chem. Commun.* **2006**, 243−256. (f) Zhou, Z.; Cao, C.; Liu, Q.; Jiang, R. *Org. Lett.* **2010**, *12*, 1780−1783. (g) Zhou, Z.; Liu, Q.; Yan, Z.; Long, G.; Zhang, X.; Cao, C.; Jiang, R. *Org. Lett.* **2013**, *15*, 606−609.

(3) (a) Wijesekera, T.; Matsumoto, A.; Dolphin, D.; Lexa, D. *Angew. Chem., Int. Ed. Engl.* **1990**, *29*, 1028−1030. (b) Dolphin, D.; Traylor, T. G.; Xie, L. Y. *Acc. Chem. Res.* **1997**, *30*, 251−259. (c) Goudriaan, P. E.; Kuil, M.; Jiang, X.-B.; van Leeuwen, P. W. N. M.; Reek, J. N. H. *Dalton Trans.* **2009**, 1677−1686. (d) Korotchenko, V. N.; Severin, K.; Gagné, M. R. *Org. Biomol. Chem.* **2008**, *6*, 1961−1965. (e) Lu, H.-J.; Jiang, H.-L.; Wojtas, L.; Zhang, X. P. *Angew. Chem., Int. Ed.* **2010**, *49*, 10192−10196. (f) de Visser, S. P.; Valentine, J. S.; Nam, W. *Angew. Chem., Int. Ed.* **2010**, *49*, 2099−2101. (g) Araghi, M.; Mirkhani, V.; Moghadam, M.; Tangestaninejad, S.; Mohammdpoor-altork, I. *Dalton Trans.* **2012**, *41*, 3087−3094.

(4) (a) Bessho, T.; Zakeeruddin, S. M.; Yeh, C.-Y.; Diau, E. W.-G.; Grätzel, M. *Angew. Chem., Int. Ed.* **2010**, *49*, 6646−6649. (b) Wu, S.-L.; Lu, H.-P.; Yu, H.-T.; Chuang, S.-H.; Chiu, C.-L.; Lee, C.-W.; Diau, E. W.-G.; Yeh, C.-Y. *Energy Environ. Sci.* **2010**, *3*, 949−955. (c) Lee, C.-W.; Lu, H. P.; Lan, C. M.; Huang, Y. L.; Liang, Y. R.; Yen, W. N.; Liu, Y. C.; Lin, Y. S.; Diau, E. W.-G.; Yeh, C. Y. *Chem.—Eur. J.* **2009**, *15*, 1403−1412. (d) Yella, A.; Lee, H.-W.; Tsao, H. N.; Yi, C.; Chandiran, A. K.; Nazeeruddin, Md. K.; Diau, E. W.-G.; Yeh, C.-Y.; Zakeeruddin, S. K.; Grätzel, M. *Science* **2011**, *334*, 629−634. (e) Subbaiyan, N. K.; D'Souza, F. *Chem. Commun.* **2012**, *48*, 3641−3643. (f) Li, L.-L.; Diau, E. W.-G. *Chem. Soc. Rev.* **2013**, *42*, 291−304.

(5) (a) Ethirajan, M.; Chen, Y.; Joshi, P.; Pandey, R. K. *Chem. Soc. Rev.* **2011**, *40*, 340−362. (b) Pandey, R. K. *J. Porphyrins Phthalocyanines* **2000**, *4*, 368−373. (c) Bonnett, R. *Chem. Soc. Rev.* **1995**, 19−33. (d) Gros, C. P.; Eggenspiller, A.; Nonat, A.; Barbe, J.-M.; Denat, F. *Med. Chem. Commun.* **2011**, *2*, 119−125. (e) Bříza, T.; Králová, J.; Cígler, P.; Kejík, Z.; Poučková, P.; Vašek, P.; Moserová, I.; Martásek, P.; Král, V. *Bioorg. Med. Chem. Lett.* **2012**, *1*, 82−84. (f) Kumar, D.; Mishra, B. A.; Shekar, K. P. C.; Kumar, A.; Akamatsu, K.; Kusaka, E.; Ito, T. *Chem. Commun.* **2013**, *49*, 683−685.

(6) (a) Zhang, J.; Li, Y.; Yang, W.; Lai, S.-W.; Zhou, C.; Liu, H.; Che, C.-M.; Li, Y. *Chem. Commun.* **2012**, *48*, 3602−3604. (b) Rakow, N. A.; Suslick, K. S. *Nature* **2000**, *406*, 710−713. (c) Suslick, K. S. *MRS Bull.* **2004**, *29*, 720−725. (d) Zhang, C.; Suslick, K. S. *J. Am. Chem. Soc.* **2005**, *127*, 11548−11549. (e) Zhang, C.; Bailey, D. P.; Suslick, K. S. *J. Agric. Food Chem.* **2006**, *54*, 4925−4931. (f) Suslick, K. S.; Rakow, N. A.; Kosal, M. E.; Chou, J.-H. *J. Porphyrins Phthalocyanines* **2000**, *4*, 407−413. (g) Musto, C. J.; Lim, S. H.; Suslick, K. S. *Anal. Chem.* **2009**, *81*, 6526−6533. (h) Feng, L.; Musto, C. J.; Kemling, J. W.; Lim, S. H.; Zhong, W.; Suslick, K. S. *Anal. Chem.* **2010**, *82*, 9433−9440. (i) Askim, J. R.; Mahmoudi, M.; Suslick, K. S. *Chem. Soc. Rev.* **2013**, *42*, 8649−8682.

(7) (a) Senge, M. O.; Fazekas, M.; Notaras, E. G. A.; Blau, W. J.; Zawadzka, M.; Locos, O. B.; Mhuircheartaigh, E. M. N. *Adv. Mater.* **2007**, *19*, 2737−2774. (b) de la Torre, G.; Vázquez, P.; Agulle-Lapez, F.; Torres, T. *Chem. Rev.* **2004**, *104*, 3723−3750. (c) Zakavi, S.; Omidyan, R.; Ebrahimi, L.; Heidarizadi, F. *Inorg. Chem. Commun.* **2011**, *14*, 1827−1832. (d) Kalnoor, B. S.; Bist, P. B.; Jena, K. C.; Velkannan, V.; Bhyrappa, P. *J. Phys. Chem. A* **2013**, *117*, 8216−8221. (e) Senge, M. O.; Fazekas, M.; Pintea, M.; Zawadzka, M.; Blau, W. J. *Eur. J. Org. Chem.* **2011**, 5797−5816. (f) Notaras, E. G. A.; Fazekas, M.; Doyle, J. J.; Blau, W. J.; Senge, M. O. *Chem. Commun.* **2007**, 2166−2168. (g) Zawadzka, M.; Wang, J.; Werner J. Blau, W. J.; Senge, M. O. *Photochem. Photobiol. Sci.* **2013**, *12*, 996−1007. (h) Wang, A.; Long, L.; Meng, S.; Li, X.; Zhao, W.; Song, Y.; Cifuentes, M. P.; Humphrey, M. G.; Zhang, C. *Org. Biomol. Chem.* **2013**, *11*, 4250−4257.

(8) (a) Kosal, M. E.; Chou, J.-H.; Wilson, S. R.; Suslick, K. S. *Nat. Mater.* **2002**, *1*, 118−121. (b) Suslick, K. S.; Bhyrappa, P.; Chou, J. H.; Kosal, M. E.; Nakagaki, S.; Smithenry, D. W.; Wilson, S. R. *Acc. Chem. Res.* **2005**, *38*, 283−291.

(9) (a) Giraudeau, A.; Callot, H. J.; Jordan, J.; Ezhar, I.; Gross, M. *J. Am. Chem. Soc.* **1979**, *101*, 3857−3862. (b) Giraudeau, A.; Callot, H. J.; Gross, M. *Inorg. Chem.* **1979**, *18*, 201−206.

(10) (a) Medforth, C. J.; Senge, M. O.; Smith, K. M.; Sparks, L. D.; Shelnut, J. A. *J. Am. Chem. Soc.* **1992**, *114*, 9859−9869. (b) Retsek, J. L.; Medforth, C. J.; Nurco, D. J.; Gentemann, S.; Chirvony, V. S.; Smith, K. M.; Holten, D. *J. Phys. Chem. B* **2001**, *105*, 6396−6411. (c) Kadish, K. M.; Royal, G.; Van Caemelbecke, E.; Gueletti, L. In *The Porphyrin Handbook*; Kadish, K. M., Smith, K. M., Guilard, R., Eds.; Academic Press: San Diego, 2000; Vol. *9*, pp 1−219.

(11) (a) Hombrecher, H. K.; Gherdan, V. M.; Ohm, S.; Cavaleiro, J. A. S.; Neves, M. G. P. M. S.; Condesso, M. F. *Tetrahedron* **1993**, *49*, 8569−8578. (b) Vicente, M. G. H; Neves, M. G. P. M. S.; Cavaleiro, J. A. S.; Hombrecher, H. K.; Koll, D. *Tetrahedron Lett.* **1996**, *37*, 261−262. (c) Shea, K. M.; Jaquinod, L.; Smith, K. M. *J. Org. Chem.* **1998**, *63*, 7013−7021. (d) Catalano, M. M.; Crossley, M. J.; Harding, M. M.; King, L. G. *J. Chem. Soc., Chem. Commun.* **1984**, 1535−1536. (e) Crossley, M. J.; Harding, M. M.; Tansey, C. W. *J. Org. Chem.* **1994**, *59*, 4433−4437.

(12) (a) Bartoli, J. F.; Mansuy, O.; Le, B.-O.; Ozette, K. L. B.; Palacio, M.; Mansuy, D. *J. Chem. Soc., Chem. Commun.* **2000**, 827−828. (b) Chirvony, V. S.; van Hoek, A.; Schaafsma, T. J.; Pershukevich, P. P.; Filatov, I. V.; Avilov, I. V.; Shishporenok, S. I.; Terekhov, S. N.; Malinovskii, V. L. *J. Phys. Chem. B* **1998**, *102*, 9714−9724. (c) Sen, A.; Krishnan, V. *Tetrahedron Lett.* **1996**, *37*, 5421−5424.

(13) (a) Callot, H. J. *Bull. Soc. Chim. Fr.* **1974**, 1492−1496. (b) Crossley, M. J.; Burn, P. L.; Chew, S. S.; Cuttance, F. B.; Newsom, I. A. *J. Chem. Soc., Chem. Commun.* **1991**, 1564−1566. (c) Crossley, M. J.; Burn, P. L.; Langford, S. J.; Pyke, S. M.; Stark, A. G. *J. Chem. Soc., Chem. Commun.* **1991**, 1567−1568. (d) Bakar, M. A.; Sergeeva, N. N.; Juillard, T.; Senge, M. O. *Organometallics* **2011**, *30*, 3225−3228.

(e) Pereira, A. M. V. M; Richeter, S.; Jeandona, C.; Gisselbrechta, J.-P.; Wytkoa, J.; Ruppert, R. *J. Porphyrins Phthalocyanines* **2012**, *16*, 465−478. (f) Lewtak, J. P.; Gryko, D. T. *Chem. Commun.* **2012**, *48*, 10069−10086. (g) Ali, H.; Van Lier, J. E. *Tetrahedron* **1994**, *50*, 11933−11944. (h) Locos, O. B.; Arnold, D. P. *Org. Biomol. Chem.* **2006**, *4*, 902−916. (i) DiMagno, S. G.; Lin, V. S. Y.; Therien, M. J. J. *Am. Chem. Soc.* **1993**, *115*, 2513−2515. (j) Liu, Y.; Xiang, N.; Feng, X.; Shen, P.; Zhou, W.; Weng, C.; Zhao, B.; Tan, S. *Chem. Commun.* **2009**, 2499−2501. (k) Odobel, F.; Suzenet, F.; Blart, E.; Quintard, J.-P. *Org. Lett.* **2000**, *2*, 131−133. (l) Rai, S.; Ravikanth, M. *J. Org. Chem.* **2008**, *73*, 8364−8375. (m) Sergeeva, N. N.; Scala, A.; Bakar, M. A.; O'Riordan, G.; O'Brien, J.; Grassi, G.; Senge, M. O. *J. Org. Chem.* **2009**, *74*, 7140−7147. (n) Frampton, M. J.; Akdas, H.; Cowley, A. R.; Rogers, J. E.; Slagle, J. E.; Fleitz, P. A.; Drobizhev, M.; Rebane, A.; Anderson, H. L. *Org. Lett.* **2005**, *7*, 5365−5368.

(14) (a) Drain, C. M.; Varotto, A.; Radivojevic, I. *Chem. Rev.* **2009**, *109*, 1630−1658. (b) Beletskaya, I. P.; Tyurin, V. S.; Tsivadze, A. Yu.; Guilard, R.; Stern, C. *Chem. Rev.* **2009**, *109*, 1659−1713.

(15) (a) Wang, Q.; Campbell, W. M.; Bonfantani, E. E.; Jolley, K. W.; Officer, D. L.; Walsh, P. J.; Gordon, K.; Humphry-Baker, R.; Nazeeruddin, M. K.; Grätzel, M. *J. Phys. Chem. B* **2005**, *109*, 15397−15409. (b) Campbell, W. M.; Jolley, K. W.; Wagner, P.; Wagner, K.; Walsh, P. J.; Gordon, K. C.; Schmidt-Mende, L.; Nazeeruddin, M. K.; Wang, Q.; Grätzel, M.; Officer, D. L. *J. Phys. Chem. C* **2007**, *111*, 11760−11762. (c) Morone, M.; Beverina, L.; Abbotto, A.; Silvestri, F.; Collini, E.; Ferrante, C.; Bozio, R.; Pagani, G. A. *Org. Lett.* **2006**, *8*, 2719−2723.

(16) (a) Renner, M. W.; Furenlid, L. R.; Barkigia, K. M.; Forman, A.; Shim, H.-K.; Smith, K. M.; Fajer, J. *J. Am. Chem. Soc.* **1991**, *113*, 6891−6898. (b) Furenlid, L. R.; Renner, M. W.; Fajer, J. *J. Am. Chem. Soc.* **1990**, *112*, 8987−8989. (c) Barkigia, K. M.; Renner, M. W.; Furenlid, L. R.; Medforth, C. J.; Smith, K. M.; Fajer, J. *J. Am. Chem. Soc.* **1993**, *115*, 3627−3635. (d) Sparks, L. D.; Medforth, C. J.; Park, M.-S.; Chamberlain, J. R.; Ondrias, M. R.; Senge, M. O.; Smith, K. M.; Shelnutt, J. A. *J. Am. Chem. Soc.* **1993**, *115*, 581−592. (e) Shelnutt, J. A.; Medforth, C. J.; Berber, M. D.; Barkigia, K. M.; Smith, K. M. *J. Am. Chem. Soc.* **1991**, *113*, 4077−4087. (f) Senge, M. O.; Medforth, C. J.; Sparks, L. D.; Shelnutt, J. A.; Smith, K. M. *Inorg. Chem.* **1993**, *32*, 1716−1723. (g) Renner, M. W.; Barkigia, K. M.; Zhang, Y.; Medforth, C. J.; Smith, K. M.; Fajer, J. *J. Am. Chem. Soc.* **1994**, *116*, 8582−8592. (h) Harada, R.; Matsuda, Y.; Okawa, H.; Kojima, T. *Angew. Chem., Int. Ed.* **2004**, *43*, 1825−1828. (i) Kojima, T.; Harada, R.; Nakanishi, T.; Kaneko, K.; Fukuzumi, S. *Chem. Mater.* **2007**, *19*, 51−58.

(17) (a) Mandon, D.; Ochsenbein, P.; Fisher, J.; Weiss, R.; Jayaraj, K.; Austin, R. N.; White, P. S.; Brigaud, O.; Battioni, P.; Mansuy, D. *Inorg. Chem.* **1992**, *31*, 2044−2049. (b) Hodge, J. A.; Hill, M. G.; Gray, H. B. *Inorg. Chem.* **1995**, *34*, 809−812.

(18) (a) Ochsenbein, P.; Ayougou, K.; Mandon, D.; Fischer, J.; Weiss, R.; Austin, R. N.; Jayaraj, K.; Gold, A.; Terner, J.; Fajer, J. *Angew. Chem., Int. Ed. Engl.* **1994**, *33*, 348−350. (b) D'Souza, F.; Zandler, M.; Tagliatesta, P.; Ou, Z.; Shao, J.; Van Caemelbecke, E.; Kadish, K. M. *Inorg. Chem.* **1998**, *37*, 4567−4572.

(19) Collini, E.; Mazzucato, S.; Zerbetto, M.; Ferrante, C.; Bozio, R.; Pizzotti, M.; Tessore, F.; Ugo, R. *Chem. Phys. Lett.* **2008**, *454*, 70−74.

(20) Liu, Z.-B.; Tian, J.-G.; Guo, Z.; Ren, D.-M.; Du, F.; Zheng, J.-Y.; Chen, Y.-S. *Adv. Mater.* **2008**, *20*, 511−515.

(21) (a) Senge, M. O.; Gerstung, V.; Ruhlandt-Senge, K.; Runge, S.; Lehmann, I. *J. Chem. Soc., Dalton Trans.* **1998**, 4187−4199. (b) Duval, H.; Bulach, V.; Fischer, J.; Weiss, R. *Inorg. Chem.* **1999**, *38*, 5495−5501. (c) Jaquinod, L.; Khoury, R. G.; Shea, K. M.; Smith, K. M. *Tetrahedron* **1999**, *5*, 13151−13158. (d) Leroy, J.; Porhiel, E.; Bondon, A. *Tetrahedron* **2002**, *58*, 6713−6722. (e) Bhyrappa, P.; Sankar, M.; Varghese, B. *Inorg. Chem.* **2006**, *45*, 4136−4149. (f) Bhyrappa, P.; Arunkumar, C.; Varghese, B. *Inorg. Chem.* **2009**, *48*, 3954−3965. (g) Chen, J.; Li, K.-L.; Guo, Y.; Liu, C.; Guo, C.-C.; Chen, Q.-Y. *RSC Adv.* **2013**, *3*, 8227−8231. (h) Fang, Y.; Bhyrappa, P.; Ou, Z.; Kadish, K. M. *Chem.—Eur. J.* **2014**, *20*, 524−532.

(22) (a) Adler, A. D.; Longo, F. R.; Kampas, F.; Kim, J. *J. Inorg. Nucl. Chem.* **1970**, *32*, 2443−2445. (b) Scheidt, W. R.; Lee, Y. J. *Struct. Bonding (Berlin)* **1987**, *64*, 1−70. (c) Scheidt, W. R. In *The Porphyrin Handbook*; Kadish, K. M., Smith, K. M., Guilard, R., Eds.; Academic Press: New York, 2000; Vol. 3, pp 49−112.

(23) (a) Ghosh, A. *Acc. Chem. Res.* **1998**, *31*, 189−198. (b) Ghosh, A. In *The Porphyrin Handbook*; Kadish, K. M., Guilard, R., Smith, K. M., Eds.; Academic Press: San Diego, CA, 1999; Vol. 7, pp 1−38. (c) Ghosh, A.; Steene, E. *J. Biol. Inorg. Chem.* **2001**, *6*, 739−752. (d) Ghosh, A.; Taylor, P. R. *Curr. Opin. Chem. Biol.* **2003**, *91*, 113−124. (e) Ghosh, A. *J. Biol. Inorg. Chem.* **2006**, *11*, 712−724. (f) Thomas, K. E.; Wasbotten, I. H.; Ghosh, A. *Inorg. Chem.* **2008**, *47*, 10469−10478. (g) Alemayehu, A. B.; Hansen, L. K.; Ghosh, A. *Inorg. Chem.* **2010**, *49*, 7608−7610.

(24) (a) Terazono, Y.; Patrick, B. O.; Dolphin, D. *Inorg. Chem.* **2002**, *41*, 6703−6710. (b) Bhyrappa, P.; Velkannan, V. *Inorg. Chim. Acta* **2012**, *387*, 64−73.

(25) Marsh, D. F.; Mink, L. M. *J. Chem. Educ.* **1996**, *73*, 1188−1190.

(26) (a) Parusal, A. B. J.; Wondimagegn, T.; Ghosh, A. *J. Am. Chem. Soc.* **2000**, *122*, 6371−6374. (b) DiMangno, S. G.; Wertsching, A. K.; Ross, C. R., II *J. Am. Chem. Soc.* **1995**, *117*, 8279−8280.

(27) Meot-Ner, M.; Adler, A. D. *J. Am. Chem. Soc.* **1975**, *97*, 5107.

(28) (a) Bhyrappa, P.; Krishnan, V. *Inorg. Chem.* **1991**, *30*, 239−245. (b) Hariprasad, G.; Dahal, S.; Maiya, B. G. *J. Chem. Soc., Dalton Trans.* **1996**, 3429−3436.

(29) (a) Takeda, J.; Ohya, T.; Sato, M. *Chem. Phys. Lett.* **1991**, *183*, 384−386. (b) Tsuchiya, S. *Chem. Phys. Lett.* **1990**, *169*, 608−616. (c) Fukuzumi, S.; Kojima, T. *J. Mater. Chem.* **2008**, *18*, 1427−1439.

(30) Haddad, R. E.; Gazeau, S.; Pecaut, J.; Marchon, J.-C.; Medforth, C. J.; Shelnutt, J. A. *J. Am. Chem. Soc.* **2005**, *125*, 1253−1268.

(31) (a) Gouterman, M. *J. Chem. Phys.* **1959**, *30*, 1139−1161. (b) Ortiz, V.; Shelnutt, J. A. *J. Phys. Chem.* **1985**, *89*, 4733−4739.

(32) (a) Retsek, J. L.; Medforth, C. J.; Nurco, D. J.; Gentemann, S.; Chirvony, V. S.; Smith, K. M.; Holten, D. *J. Phys. Chem. B* **2001**, *105*, 6396−6411. (b) Gentemann, S.; Nelson, N. Y.; Jaquinod, L.; Nurco, D. J.; Leung, S. H.; Medforth, C. J.; Smith, K. M.; Fajer, J.; Holten, D. *J. Phys. Chem. B* **1997**, *101*, 1247−1254. (c) Tsuchiya, S. *Chem. Phys. Lett.* **1990**, *169*, 608−610. (d) Li, B.; Li, J.; Fu, Y.; Bo, Z. *J. Am. Chem. Soc.* **2004**, *126*, 3430−3431.

(33) (a) Smirnov, V. V.; Woller, E. K.; DiMagno, S. G. *Inorg. Chem.* **1998**, *37*, 4971−4978. (b) Medforth, C. J.; Smith, K. M. *Tetrahedron Lett.* **1990**, *31*, 5583−5586.

(34) (a) Kadish, K. M.; Lin, X. Q.; Han, B. C. *Inorg. Chem.* **1987**, *26*, 4161−4167. (b) Kadish, K. M.; Ou, Z.; Tan, X.; Boschi, T.; Monti, D.; Fares, V.; Tagliatesta, P. *Dalton Trans.* **1999**, 1595−1601. (c) Terazono, Y.; Dolphin, D. *J. Org. Chem.* **2003**, *68*, 1892−1900. (d) Giraudeau, A.; Louati, A.; Callot, H. J.; Gross, M. *Inorg. Chem.* **1981**, *20*, 769−772.

(35) Hansch, C.; Leo, A.; Taft, R. W. *Chem. Rev.* **1991**, *91*, 165−195.

(36) Ghosh, A.; Halvorsen, I.; Nilsen, H. J.; Steene, E.; Wondimagegn, T.; Lie, R.; Van Caemelbecke, E.; Guo, N.; Ou, Z.; Kadish, K. M. *J. Phys. Chem. B* **2001**, *105*, 8120−8124.

(37) (a) Walker, F. A.; Beroiz, D.; Kadish, K. M. *J. Am. Chem. Soc.* **1976**, *98*, 3484−3489. (b) Kadish, K. M.; Morrison, M. M. *J. Am. Chem. Soc.* **1976**, *98*, 3326−3328.

(38) Takeuchi, T.; Gray, H. B.; Goddard, W. A., III *J. Am. Chem. Soc.* **1994**, *116*, 9730−9732.

(39) (a) Chan, K. S.; Zhou, X.; Lou, B.-S.; Mak, T. C. W. *J. Chem. Soc., Chem. Commun.* **1994**, 271−272. (b) Chandra, T.; Kraft, B. J.; Huffman, J. C.; Zaleski, J. M. *Inorg. Chem.* **2003**, *42*, 5158−5172.

(40) (a) Bhyrappa, P.; Velkannan, V. *J. Porphyrins Pthalocyanines* **2011**, *15*, 884−889. (b) Kojima, T.; Hanabusa, K.; Ohkubo, K.; Shiro, M.; Fukuzumi, S. *Chem. Commun.* **2008**, 6513−6515.